Reliable, Practical Kilowatt-class Cryogenics for Superconducting Devices

Final Report

SBIR Grant Number: DE-OE0000528 (Phase III)

DoE Project Manager: Debbie Haught

Recipient: Clever Fellows Innovation Consortium, Inc.
(dba CFIC-Qdrive; acquired by Chart Industries in 2012)
302 Tenth St.
Troy, NY 12180

Principal Investigator: Dr. Philip Spoor

Project Director: John Corey

Period of Performance: October 2010-April 2013

NOTICE

This report was prepared by Chart Industries in the course of performing work contracted for and sponsored by the U.S. Department of Energy (hereafter the "Sponsors"). The opinions expressed in this report do not necessarily reflect those of the Sponsors, and reference to any specific product, service, process, or method does not constitute an implied or expressed recommendation or endorsement of it. Further, the Sponsors make no warranties or representations, expressed or implied, as to the fitness for particular purpose or merchantability of any product, apparatus, or service, or the usefulness, completeness, or accuracy of any processes, methods, or other information contained, described, disclosed, or referred to in this report. The Sponsors and the contractor make no representation that the use of any product, apparatus, process, method, or other information will not infringe privately owned rights and will assume no liability for any loss, injury, or damage resulting from, or occurring in connection with, the use of information contained, described, disclosed, or referred to in this report.

SBIR/STTR RIGHTS NOTICE

These SBIR/STTR data are furnished with SBIR/STTR rights under Grant No. OE0000528. For a period of 4 years after acceptance of all items to be delivered under this grant, the Government agrees to use these data for Government purposes only, and they shall not be disclosed outside the Government (including disclosure for procurement purposes) during such period without permission of the grantee, except that, subject to the foregoing use and disclosure prohibitions, such data may be disclosed for use by support contractors. After the aforesaid 4-year period the Government has a royalty-free license to use, and to authorize others to use on its behalf, these data for Government purposes, but is relieved of all disclosure prohibitions and assumes no liability for unauthorized use of these data by third parties. This Notice shall be affixed to any reproductions of these data in whole or in part.

TABLE OF CONTENTS

LIST OF FIGURES

Executive Summary

Superconducting devices require croygenic refrigeration to sustain the temperatures that enable superconductivity, typically 30-80 Kelvin for so-called “high-temperature” superconductors. The goal of this project was to design, build, and test large-scale acoustic-Stirling cryocoolers with the new flexibly attached remote (FAR) coaxial coldfingers, as candidates for practical and reliable cooling of utility-grade systems. In this format, the coldhead is coupled to its pressure wave generator (PWG) through a hose of 1 to 2 meter length. At the inception of this project, it was thought that the combination of the coaxial coldfinger and flexible connection would enable simple and direct interfacing to most high-temperature superconductor (HTS) applications. Developing units at a nominal 1,000 watts cooling capacity (as measured at 77K) provides answers to the applications identified by DoE’s HTS Cryogenics Roadmap [1], specifically the HTS-4 specification (cables, larger devices).

As detailed in our Phase II report [2] the Roadmap’s goals were optimistic and certain of them (the cost targets) have not been achieved by anyone, even now (in 2016). However, in Phase II we did come close to reaching the HTS-3 capacity goals and came within striking distance of the efficiency goal. In this Phase III, we wound up spending almost all of our time on the coldhead development, with only partial success (although we do have a good idea of how to improve the performance further if the opportunity arose). This can largely be attributed to our decision to pursue a considerable scale-up of our Phase II coldfinger, which is already the largest coaxial pulse-tube that has been demonstrated, to our knowledge. A coaxial ‘pulse-tube’ coldfinger at such a large scale has many unique challenges relating to maintaining transverse uniformity of flow and temperature. The large size also leads to high costs for certain components, and a great deal of awkwardness in testing. We had originally planned to start with a flanged coldhead that would allow for easy swap of parts in the cold end, to help us learn iteratively how best to manage the flows in that critical zone. However, we could never get a good, repeatable cold seal, so the flanged version had to be abandoned.

The choice to pursue a single, coaxial coldhead appeared to make sense at the time, given the feedback from potential users. Many expressed a preference for applying cooling directly to the load or put the cooling surface directly in a dewar, without using intervening pipes or cryogenic pumps. However, we have since discovered that the difficulties of using external cryogenic lines and pumps are perhaps exaggerated, and a remotely-mounted large coaxial coldhead may not be an enabling technology. Furthermore, the HTS market which would in theory have demanded these large coaxial coldfingers has still not matured. The markets that do exist for what we might call “mesoscale” cooling (in the few thousand watts, not optimum for established large cooling technologies such as reverse-Brayton) are mostly in the condensing or recondensing of process gas, as in zero-boiloff storage or in liquefying natural gas at wellheads. These interface naturally with ‘inline’ coldheads that use ‘process’ heat exchangers (*e.g.* integral shell-and-tube HX’s), that are made for cooling a flow of process fluid.

Finally, we never did find good paths to low-cost manufacturing in the relatively small quantities that we considered in this program (tens of units a year, to start). While the DOE 'Roadmap' cost targets seem in retrospect to be excessively optimistic, the technology developed in this program is still too expensive for the markets that do exist. This has subsequently led us to consider very different technical approaches to supplying cooling at the HTS-4 and HTS-3 target capacities.

Accomplishments to Goals & Objectives

DoE's HTS Cryogenics Roadmap and Goals for This Project

At the inception of this project (2010) it was believed that superconducting materials had matured to the point that cryogenic cooling would soon become the bottleneck in the widespread adoption of superconducting technology. We took our lead from the DOE "Cryogenics Roadmap'' [1] developed by a consortium from industry, academia, and government as a plan for how cryogenic technology might be developed to meet the needs of the emerging HTS market, and how the government might provide targeted funding and guidance to spur this development.

The most basic goals established by the Roadmap were the following (taken directly from [1]):

1. Increase reliability to allow availability of 99.8%
   This is the availability of the cryogenic subsystem including controls. Recent feedback from industry indicates that the HTS power component itself requires 99.8-99.9 % availability: this means the cryogenic subsystem needs 99.9% and higher reliability; this is about one 8-hour shift of unavailability per year.
2. Increase efficiency to achieve 30 % of Carnot
   Some ways to increase efficiency may lower reliability: for example, going from 1 to 2 expanders in a Brayton cycle. The reliability can be increased through redundancy but this impacts front-end cost.
3. Decrease cost from $100 to $25/W at ~ 65-80 K
   The least painful way to do this is to increase the production base and use standardized components.

As mentioned earlier, the Roadmap performance goals were very challenging, but the cost targets remain even more elusive, with no company offering systems for sale that meet or exceed these targets, even in 2016. To be fair, this lack of availability is strongly influenced by the weak market for HTS cooling.

HTS-4 Objectives & Achievements

HTS-4 was the main focus of this Phase III. From [1], the specific goals for HTS-4 devices (cables, and other larger loads) are given in Table 1.

Table 1: HTS-4 system goals, from the Cryogenic Roadmap.

Parameter	Roadmap Value
Temperature Range (K)	65 – 80 K
Capacity at midpoint of range (W)	**1500 W at 72.5 K**
Capacity at low end of range (W)	**1050 W at 65 K**
% Carnot Efficiency	**25% min, 30% Goal**
Compressor/ Driver	**Oil Free**
Capital Cost $ per watt (at 80K)	**$60 max, <$40 Goal**
MTBF (hrs)	17,520
System mass kg/Watt at 65K	0.75 max, <0.5 Goal
Cryocooler Availability %	99.8% min, 99.9% Goal
Mean Time to Repair (hrs)	4

Table 2: Our Phase III system goals from our proposal, along with the outcomes achieved.

Parameter	Phase III Proposed	Phase III Achieved
Capacity at 80K (W)	**~1000 W at 20 kWe in**	650 W (at 15 kWe) (764 W extrapolated, at 20 kWe)
Capacity at 50K (W)	**~500 W at 20 kWe in**	?*
% Carnot Efficiency	**---**	11% (at 80K)
Compressor/ Driver	**Oil Free**	Oil Free
Capital Cost $ per watt (at 80K)	**<$40**	~ $130

*Anticipated performance of a coldhead that was specifically designed for enhanced performance at lower temperatures. It was simulated, and drawings were produced, but it was never built.

Note that our Phase III objectives, as outlined in our proposal, differ significantly from the HTS-4 targets. Those targets were aspirational, not necessarily practical, and we did not propose to meet all of them. The cost-per-watt target was preserved, but we did not specifically plan to meet the cost target at 65K, as the Roadmap suggests.

Obviously, we fell short of meeting the Phase III program goals. The issues with the coldhead were never fully solved, even though we continued working on it well into 2014, far beyond the official period of performance. In particular, the large coaxial coldhead appears to suffer from an anomaly called “regenerator streaming” not seen in any of our smaller coldheads, and it took considerable time to diagnose the problem and

come up with a workable solution. (We believe we finally *did* discover the solution, but we ran out of time to fully implement it.) On the cost side, there were many lower-cost strategies we pursued that did not ultimately work out. In addition, the prices of some key materials (copper and stainless steel) rose significantly from when we began the project.

We came closest on capacity; outright, we made 65% of our goal. This was at 75% of our nominal target input power; we were limited by a mismatch between the coldhead and the linear compressor (Pressure Wave Generator, or PWG) used to drive it (the acoustic impedance of the coldhead was a bit different than our simulations suggested). This could have been easily corrected in subsequent tests; we can examine the data we *do* have to estimate what capacity at 80K we might have achieved, as shown in Figure 1.

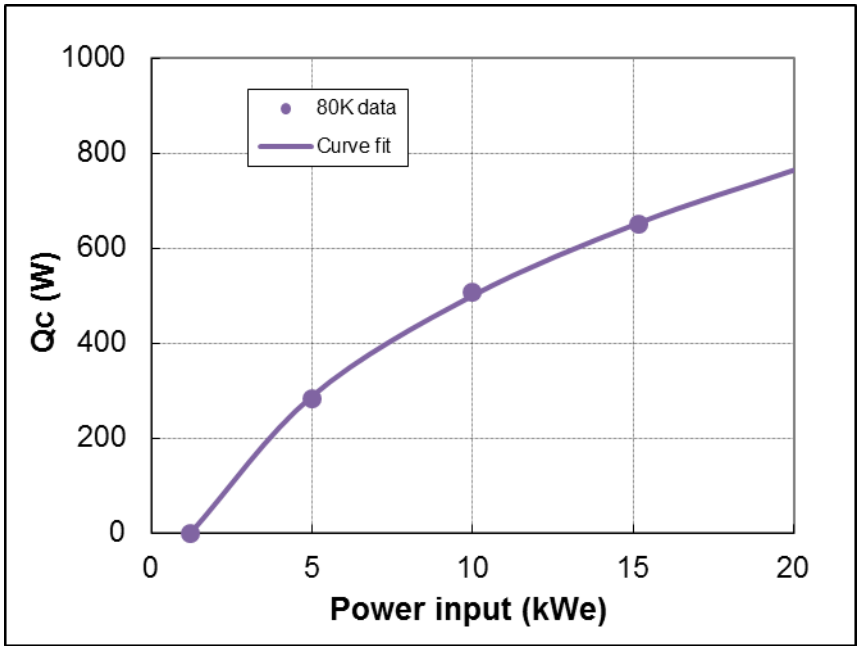

Figure 1: Cooling capacity at 80K as a function of input power for the Phase III demo system.

The cooling power is very nearly proportional to the square root of input power; in our previous (and subsequent) experience with cryocoolers, this relationship is generally much more linear. The extrapolated value at 20 kWe input is 764 W, so we can suppose that with very minor tweaks, the Phase III system would achieve 76% of the original capacity goal. However, not only is the coldhead very nonlinear with amplitude, it is also very nonlinear with coldtip temperature, performing relatively poorly at 70K and below. The coldhead troubleshooting consumed most of our experimental time and resources. Eventually we did find a way to soften these nonlinearities, but we were not able to implement it fully before time ran out.

Overall, our main lesson learned from this project was to avoid program overreach. We attempted to develop cryogenic hardware on an unprecedented scale, and at the same time find ways to reduce its cost, and that of an entire system, by over 75%, *and* build a

demonstration low-cost system, *and* get it integrated into a test site. This proved rather ambitious and spread our resources thin. We would have been better off choosing a particular emphasis (cost reduction, or scale-up) and focusing just on that. For instance, we could have used multiple "200W at 80K" coldheads to build a larger-capacity system, as in fact we did in the oxygen liquefiers we have built for the Navy. We could then have put all the effort in to cost-reduction on that system, where the 1st-order technical risk (the risk that the system would not work or would not meet capacity targets) was basically zero. Any cost-reduction strategies that were successful with these coldheads would then apply to HST-3 and HST-4 sized systems, both. Or, we could have chosen the scale-up of the smaller coldhead as the real goal, recognizing its degree of difficulty, and accepting the risk that the scale-up would not be practical, without simultaneously jeopardizing other parts of a larger program. Regardless, this project did remind us that major technical hurdles are easy to underestimate when laying out a schedule.

Coldhead design

Initial expectations

It is instructive to return to our basis for predicting the performance of the Phase III system, which we began near the end of Phase II. Although we did not formally propose to address the specific capacity goals of HTS-4, it is interesting to note that the HTS-4 goals and the predicted performance of our Phase III system were not on the same trajectory (see Figure 2). The dashed curve, obtained by offsetting the simulation by 33% of the predicted cooling power at 65K, is an empirical correction discussed in our Phase II report [2]. This correction was found to predict fairly accurately the performance of not only our Phase II system, but also that of an earlier 'in-line' prototype upon which we based some of our assumptions about Phase II. Applied to the larger cryocooler simulation at the end of Phase II, it implies that we could reasonably expect to get about half of the HTS-4 target capacity at 65K. Note also that this "–33% at 65K" rule predicts 825W at 80K, only 8% more than our extrapolated result from Figure 1. This is yet another example of this rule enabling a fairly accurate estimate of performance for real hardware, based on simulations.

As was the case with Phase II, we had data from an inline coldhead built during an earlier collaboration with Praxair to help us predict how well we might do with our scaled-up coaxial coldhead in Phase III. These data are also featured in Figure 2. The Praxair/QDrive system achieved 1100W at 77K from 24.6 kWe [3] for 13% of Carnot. The system did achieve higher efficiencies, as much as 16% of Carnot at 72K, but this was at lower input power [4]. The full-power data for this system are shown in Fig Figure 2, along with the HTS-4 targets and our simulations. The data have a lot of scatter and are in a narrow temperature range, because they are based on heat-balancing a subcooled nitrogen flow.

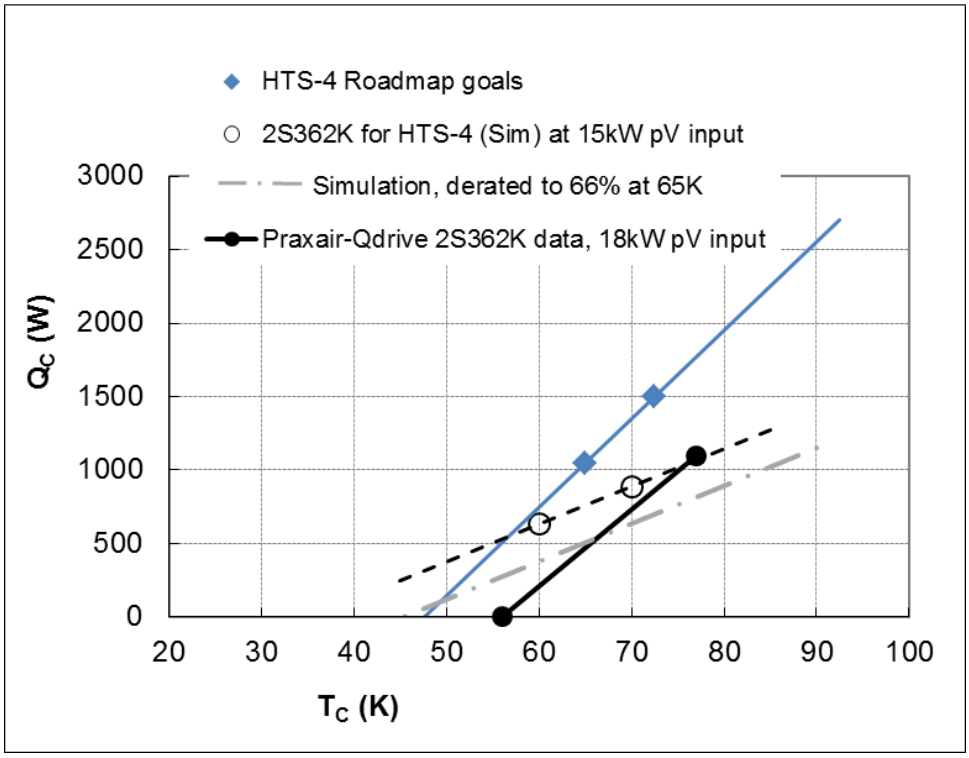

Figure 2: A (linear) cooling curve extrapolated from the HTS-4 targets, compared to the predictions of our simulation at the end of Phase II. Also featured are data from a system built with our large PWG and a close-coupled, inline coldhead from Praxair, Inc.

Hence it is hard to draw firm conclusions about the slope of the curve, although it is stated [3] that the implied stall temperature from the clustered data (~56K) is close to what they measured with a drilled copper block in place of the cold process heat exchanger. This makes the slope nearly identical to the HTS-4 goals, just offset by 700 watts.

It would be of great interest to know what a fuller characteristic of the Praxair coldhead would look like, over a larger temperature range. It is generally true that small single-stage cryocoolers tend to have very linear load curves (cooling power versus temperature) for constant input power, but there are a multitude of effects that can disrupt that relationship in large cryocoolers. For instance, it is very interesting to note that the Carnot efficiency of the Praxair system goes *down* with input power [4]; normally, with a small cryocooler, the opposite is true. The biggest parasitic loss in small cryocoolers is conduction loss, which is independent of amplitude. Larger input power therefore leads to higher net cooling, which hence leads to higher efficiency. In large cryocoolers (or poorly-built small ones) streaming in the buffer tube or regenerator is generally worse at higher amplitudes, and can exceed the losses due to conduction, reducing efficiency at high amplitudes. Regenerator streaming may be particularly bad at low temperatures [5].

System design and cooling capacity

The coldhead is part of a whole cryocooler, consisting of a resonant pressure-wave generator (PWG), the coldhead itself, and a long transfer line connecting them. This arrangement, with the coldhead remote from the PWG, is an important part of our system's novelty. The adoption of this arrangement did have certain consequences, not necessarily obvious. In particular, the separation of the coldhead and the PWG by two meters of transfer line essentially fixed the natural frequency of the system at a maximum of 50Hz, as opposed to the QDrive/Praxair system, which ran at 60Hz. This frequency reduction is important because the Phase III system uses essentially the same PWG design as the Praxair system, and a lower frequency implies lower power density. Hence, on the graph in Figure 2, note that the Praxair data are based on an acoustic power (*pV*) input of 18.5 kW (and an electric power input of 24.6 kWe), as opposed to our Phase III simulation, which assumes 15 kW of pV (from 20 kWe)—the powers in the systems are very close to a 5/6 ratio. Thus, even if we put the Praxair/Qdrive inline coldhead on the end of our transfer line, we would not be able to put as much power into it and the expected capacity would be closer to 1100×5/6 = 916 W at 77K. This is important because to meet our capacity target of 1000W at 77K, we would need to build a coaxial coldhead *more* efficient than the inline, even though the inline geometry has certain intrinsic advantages.

Someone familiar with this type of cryocooler, which uses a linear compressor (PWG) and an acoustic ('pulse-tube') coldhead, might initially be surprised that the frequency could not be boosted up to 60 Hz. The natural or resonance frequency of such a cooler is controlled by several factors, all of which are nominally within the designer's control: the amount of moving mass in the motors, the piston area (which affects the gas-spring contribution), the volumes on either side of the piston, the charge pressure, and to some extent, the coldhead design itself, which contributes to the impedance seen by the pistons. However, in this case there was very little room to adjust anything to raise the frequency. Among the constraints were:

1. The piston area was already quite large, near the limit for the type of motor construction. Larger area would also worsen some instabilities, such as piston drift (see Glossary of Terms).
2. The moving mass could not be reduced, as the magnet mass is fixed and the piston was already hollowed out as much as possible.
3. The charge pressure was already near the maximum for the PWG pressure vessel.
4. In a PWG so large, most of the stiffness balancing the moving mass comes from gas-spring forces on the pistons; in fact, the force on the pistons is mostly reactive. The coldhead design has a relatively minor effect on that impedance.
5. A long transfer line, however, moves the pistons "farther away" acoustically as well as physically from the coldhead, reducing the pressure wave, and hence the gas-spring force, at their location.

6. Redesigning the linear motors themselves would have been outside the scope of this project, but it is worth noting that these are about as large as we judge practical. One way around the power limitation would be to simply build bigger motors with more power at the same frequency, but the existing motors are thermally limited already—that is, it is already a challenge to remove waste heat from them effectively. Going up in size would exacerbate this further.

Therefore, we are essentially stuck with 50Hz as a ceiling for the system frequency, which lowers the achievable capacity.

Starting point: sizing of coldhead

Power density also plays a role in the design of an acoustic coldhead. To reach the capacity targets of Phase III, we found that the most efficient designs in simulation resembled the power density of our smaller coldheads. However, because the length of the components in an acoustic coldhead are more or less determined by frequency, gas type, and temperature span, the coldheads have to increase in area and decrease in aspect ratio as they go up in power. The decreasing aspect ratio *l/d* makes flow management increasingly challenging.

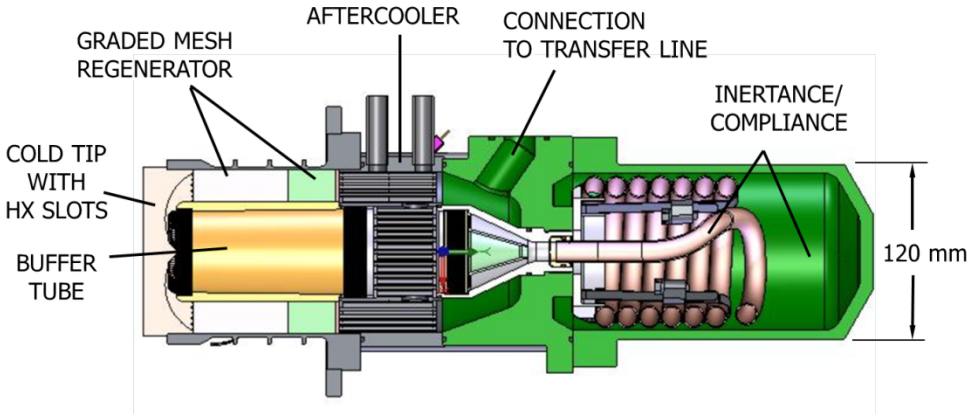

Figure 3: Cross-section of the "2S226K" coldhead, our most efficient to date, showing major components.

As an illustration, consider our most efficient coldhead type to date, the "2S226K" size (so-called because it was designed to match our PWG that uses the 226 mm-frame motors), shown in Figure 1. This coldhead achieves 150W at 77K from 2000W of input *pV* power, and has a major diameter of 120 mm. This gives it a power density, or perhaps more properly an intensity, of 1.3 W/cm^2 thermal and 17.7 W/cm^2 acoustic. The input power and cooling power are just about a factor of 10 lower than the requirements for the Phase III system; to preserve the same power density, the Phase III coldhead would have to have a major diameter of ~$\sqrt{10}$ times that of the 2S226K coldhead, or about 400 mm. The length of the coldhead, meanwhile, can't be extended very far (it is limited by the viscous pressure drop in the regenerator). At this diameter, the coldhead is considerably wider than it is tall (see schematic illustration in Figure 4). Even the buffer tube, which has to have a minimum volume to ensure there are at least several particle displacements between the warm and cold ends, will wind up being wider than it is tall.

This seems especially risky considering the coaxial geometry requires the flow to make a 180-degree turn just before entering the buffer tube. In addition, a coldhead that size would be massive and very expensive.

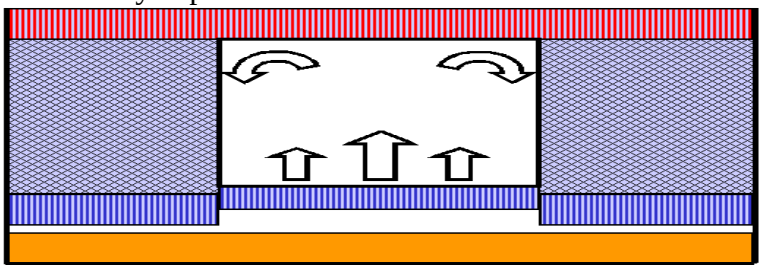

Figure 4: Schematic representation of a coldfinger with a major diameter 4× the regenerator length. The arrows suggest how an unevenly distributed flow at the cold end (possibly as a result of the abrupt turnaround) could drive convection in the buffer tube.

We wound up choosing to limit the size of the coldhead so that the buffer tube could be at least as long as tall, and have at least four or five particle displacements between the ends. When the coldhead flow area is reduced, the pressure wave amplitude (the other half of *pV* power) must be increased to compensate. On this front, we decided to limit the pressure wave amplitude to less than 5 bar peak, or about a 17% wave on a 30-to-32 bara mean. Such large pressure waves, and larger, are not uncommon in true Stirling coolers, but they can be risky in 'pulse-tube' coolers, where uniform, 'plug' flow is enforced only by acoustic elements, susceptible to turbulence and streaming. Together, these constraints (buffer tube $l/d \geq 1$, $p_1 < 5$ bar, pk) determined the approximate size of the coldhead. The OD of RGR is 180mm, the BT wound up having *l/d* just under unity; 80mm/90mm.

It's important to note here that any of the assumptions made during this sizing exercise could be challenged. Perhaps still higher power density, based on higher pressure-wave amplitude, would work fine. Perhaps the buffer-tube could be designed with merely three or even two particle displacements without the cold and warm ends communicating. Perhaps a much smaller *l/d* ratio would be fine[1]. With a new design, at a record scale, we were inclined to be cautious.

It is also worthwhile here to comment on the essential differences between acoustic-Stirling, or 'pulse-tube' coolers, and true Stirling coolers that have mechanical displacers.

[1] Both the medium (300W@77K) and large (1100W@77K) in-line coldheads we built with Praxair had buffer tubes with $l/d < 1$; the medium-sized head had $l/d \sim 0.65$ and the larger one $l/d \sim 0.53$. The small aspect ratios were a direct consequence of a decision to make all the main coldhead elements have the same diameter. Normally the buffer tubes are made a smaller diameter than the regenerator and longer; too much volume in the buffer tube will make it harder to achieve good cycle phasing and will increase the buffer tube losses. So the optimum volume requires the buffer tube be rather short, if it is made the same diameter as the regenerator. This uniformity has a distinct advantage for an inline head, as there are no area transitions between elements to disrupt the flow. For a coaxial coldhead, however, it makes the flow management worse, not better. It is worth noting, also, that the medium-sized Praxair system achieved much higher efficiency (19% of Carnot) at its highest cooling powers than did the large Praxair coldhead. Perhaps even with a uniform diameter in an inline head, there is a practical limit to *l/d*.

It has been suggested[2] that 'pulse-tube' coolers can come close to equaling the efficiency of Stirling coolers at large scales, especially at low temperatures. Stirling coolers recycle the acoustic power that passes through the thermal core, whereas 'pulse-tubes' do not; but this is a small fraction of the total *pV* power. Also, at small scales, the inertance tubes that are used to control the phasing and the amplitude of the flow on the cold end of the thermal core are not able to achieve ideal cycle phasing, because they have too much intrinsic viscous resistance. But at large scales, the decreasing surface-to-volume ratio means that the flow inertia and the viscous resistance can be chosen to have the ideal balance, and in theory can enforce ideal cycle phasing. However, no large pulse-tube cooler has come close to achieving the kind of efficiencies claimed for large Stirling coolers, which are said to equal or exceed 30% of Carnot even at 77K [6]. Even in *simulation*, it is a struggle to create a pulse-tube cooler with 30% of Carnot at 77K.

The author has observed through exercise of the simulation code "Sage" [7] that the exact same "thermal core" (heat exchangers sandwiching a regenerator) has a much higher efficiency with a mechanical displacer at the cold end than with a buffer tube, even when the impedance at the warm end of the buffer tube is allowed to be optimum without regard to whether it corresponds to a realizable inertance tube (as one can do in simulation). It is not the cycle-phasing limitation of the inertance tube versus the displacer, but rather the adiabatic volume separating the phase control from the cold heat exchanger that limits the efficiency of the 'pulse-tube' coldhead. To a first approximation, of course, displacers have losses analogous to those in a buffer tube; *e.g.* buffer tubes have Rayleigh streaming [8], while displacers have shuttle loss [9]. However, it seems that at very high pressure-wave amplitudes, the losses in buffer tubes become prohibitive much sooner than do those associated with (well-designed) displacers. It is well understood [9] that there is an ideal pressure ratio for a Stirling cycle for a given temperature ratio, and for the large temperature ratios of Stirling or acoustic-Stirling cryocoolers, that ideal ratio is simply not practical for the acoustic version.

Optimizing coldhead designs for 70K and 50K

Even as we began optimizing our simulation and designing parts, we understood that HTS technology was not quite keeping pace with the goals of the Roadmap, and if HTS were to be widely deployed there would be demand for cryocooling at temperatures below 65K. Also, we knew from our previous experience designing medium-sized coldheads that optimizing a simulation for a temperature below one's true target increased the odds of achieving good results at that target in real hardware.

We chose to pursue two designs, one nominally optimized for 50K and one for 70K. The "70K" coldhead was intended for our anticipated commercial markets outside HTS, which for the most part involve much higher process temperatures than HTS (zero boiloff storage for argon, on-site liquefaction of natural gas, etc.). The "50K" coldhead would

[2]The author has suggested it, along with others in his acquaintance.

specifically address the HTS market (should one develop) and might also serve some commercial markets. As the simulation exercise progressed, we chose to optimize the coldhead for capacity at *30K*, rather than 50K, for two reasons:

1. Experience has shown us that if large coldheads underperform their simulations, the shortfall in cooling capacity is always proportionally worse at lower temperatures.
2. The spread between 50K and 70K isn't really large enough to make a meaningful distinction in hardware.

Optimizing for 30K provides some assurance that the coldhead will perform decently at 50K (though at the expense of some theoretical capacity at 50K); however, it is reaching the limits of a high-frequency single-stage design, especially if exotic (*i.e.* expensive) regenerator materials are excluded from consideration. The extreme low temperatures and resulting high density of the helium in the cold end cause its volumetric heat capacity to approach and then surpass that of stainless steel at around 20K. Bear in mind that the regenerator is also not solid but 70% to 80% void volume, depending on what material is used. Thus, the regenerator can't provide its primary function of regenerating sensible heat isothermally. Figure 5 shows how the predicted capacity of the coldhead arcs downward just about where the heat capacities of helium versus SS cross over:

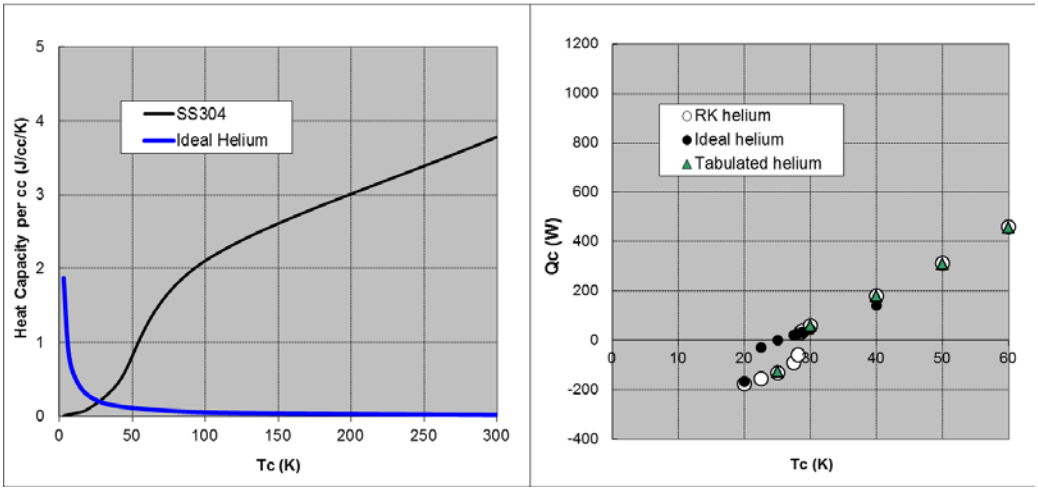

Figure 5: (left) The heat capacity of helium vs. stainless steel, versus temperature; (right) the collapse of cooling power in the coldhead simulation (using a plain SS regenerator) where these heat capacities cross. The simulation is shown for three different helium options available in Sage—"Tabulated" and "RK" include more real-fluid effects that apply at high density.

The '50K' design that resulted from the '30K' optimization did, as expected, have superior predicted performance at low temperatures, and a lower ultimate temperature, but had a gentler slope and less expected capacity at higher temperatures. Figure 6 shows the predicted performance of both coldhead designs, at the end of the simulation and analysis period (the figure distinguishes between them by regenerator length, though there are other more minor differences).

Again, the choice to bias the "50K" coldhead toward 30K was a balance of risk, accepting slightly lower predicted capacity in order to lower the risk of secondary flows. This was done mainly by making the "50K" coldhead longer than the "70K" version, but the same diameter, hence a larger aspect ratio. We looked forward to learning a great deal from comparing the actual performances of these coldheads with their predictions, as a way of understanding the practical limits of aspect ratio in 'pulse tube' coolers.

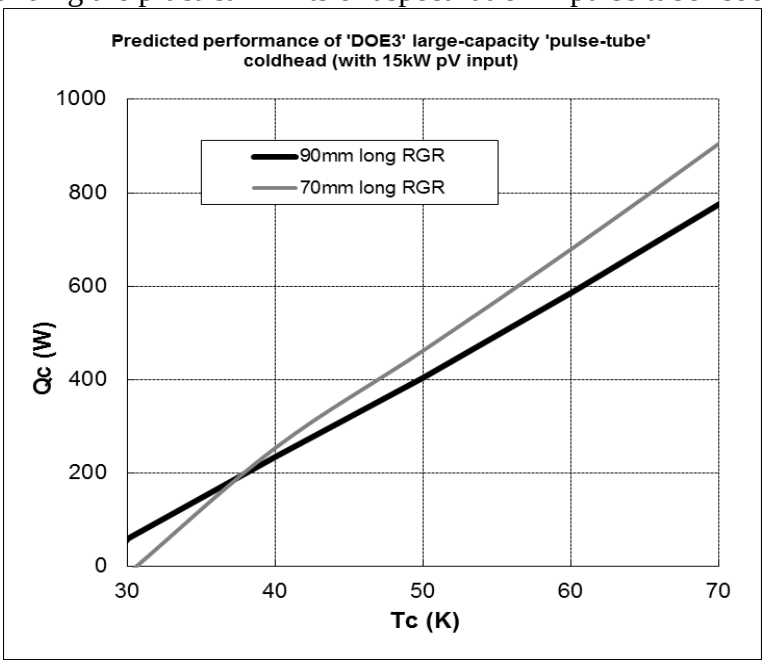

Figure 6: Predicted performance of coldhead optimized for 50K (70mm regenerator) versus the version optimized for 30K (90mm regenerator).

The construction of the 70K and 50K heads are very similar, except for a few critical dimensions. Figure 7 shows the "70K" head in cross-section, and Figure 8 shows a solid model of the whole cryocooler.

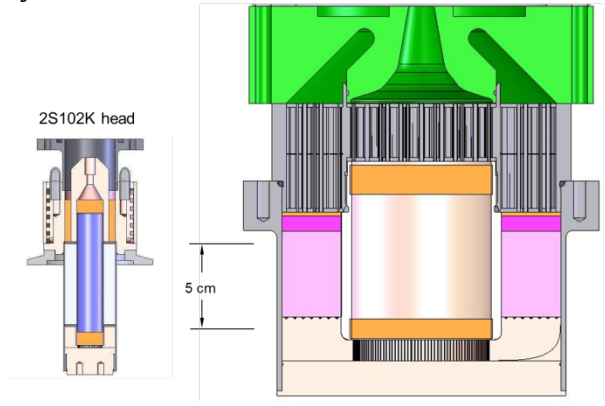

Figure 7: Cross-section of "70K" 2S362K coldhead solid model, next to the 2S102K, illustrating the change in aspect ratio with capacity.

The 70K coldhead parts were in late-stage refinement or already procured when we were still working on the 50K head design, and the experience of building the 70K coldhead motivated us to refine some of the 50K parts further. The best example is

probably the cold heat exchanger. In the 70K CHX, we tried to mimic the same manufacturing techniques that we had used on the corresponding part in the '241' coldhead, by sawing slots. However, the larger diameter made the process even more difficult, resulting in even more broken saw blades and damaged channels.

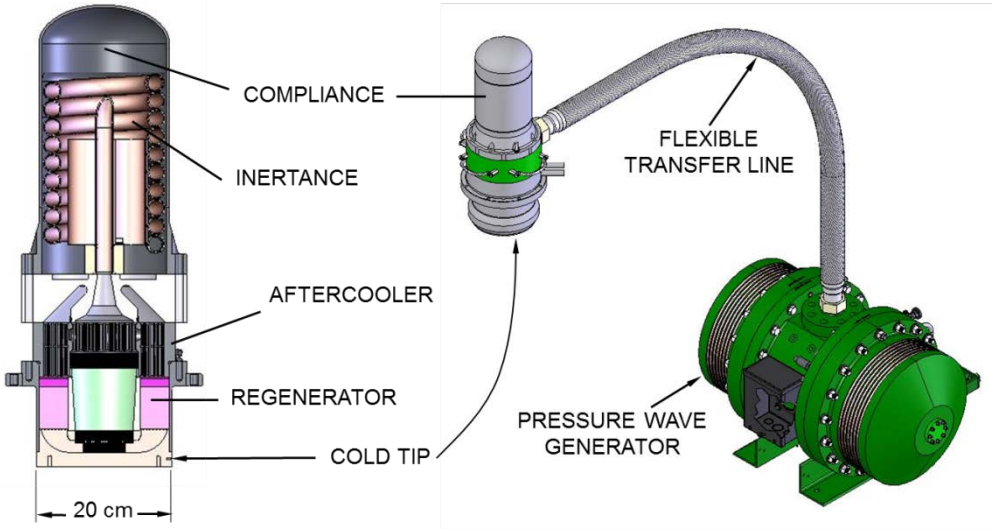

Figure 8: Solid model of entire 2S362K-FAR cryocooler, major components labeled. Coldhead is shown with integral compliance tank and inertance tube.

The CHX in a large coaxial coldhead is a challenge because the channel diameter is optimally very narrow, yet very uniform (flow resistance goes as the cube of the channel width, so even small differences can cause nonuniform flow through the array of channels). Moreover, the material must be highly conductive, yet either brazeable or weldable to stainless steel. This essentially makes copper the only good material option, but of course copper is hard to machine, and becomes very soft after brazing. This makes it easy for a fine array of slots and fins to be damaged during handling after the CHX is brazed to the SS regenerator housing. There are, of course, other lower-cost, more robust options, such as press-fitting an aluminum fin array into a drawn stainless vessel. We have used such techniques in our small, lower-cost coldheads. However, in this case, we could not take the performance penalty this kind of construction would impose.

We brainstormed and sketched and modeled many other means of producing a radial array of uniform thin slits in a thick copper disk, including the one shown in Figure 9 (an array of wedges that interlock, and are ultimately brazed to a parent disk). This design had the advantage of forming the slots as gaps between interlocking pieces, rather than trying to remove thin slices of material as with a saw blade. However, holding the tolerances on the interlocking parts well enough to make the slots uniform, and controlling the flow of braze alloy when joining the parts together, made this construction just as challenging and at least as expensive as the saw-cut version. We considered other constructions, such as a diffusion-bonded packing of small copper spheres. Ultimately, we chose an array of saw-cut slots, but accepted the performance penalty of making the slots 0.032" (1/32") wide instead of 0.020", and using fewer of them. We received one

of these cold-tip parts, but used it in a "70K" coldhead brazement (more on that in "Coldhead Assembly and Testing"). Figure 10 shows the original and the simplified CHXs.

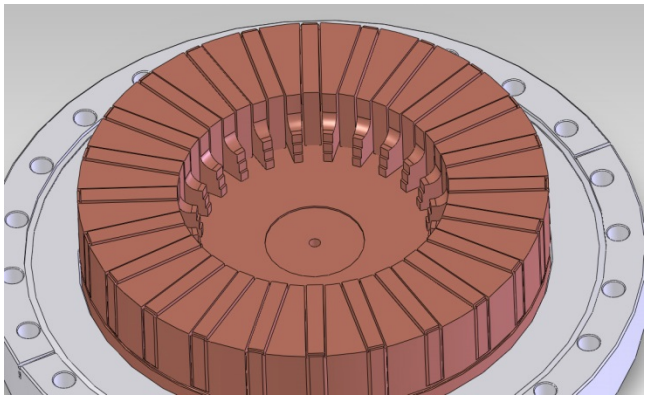

Figure 9: Rendering of CHX comprising a radial array of interlocking wedges, all brazed together.

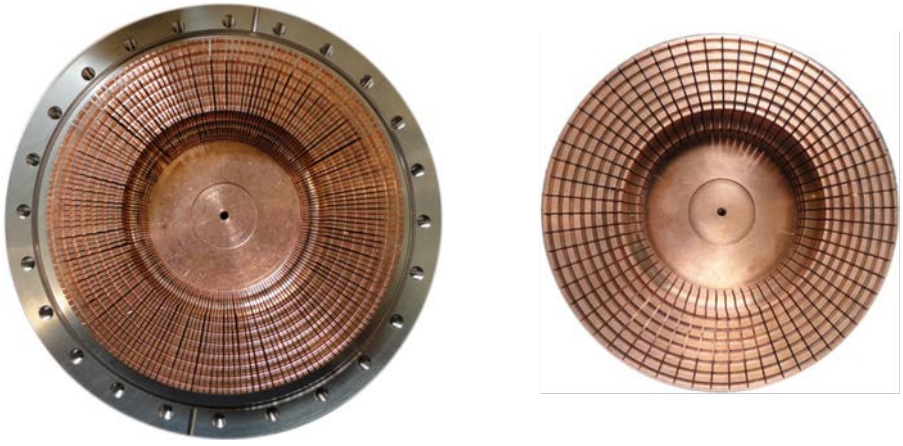

Figure 10: (Left) Original CHX for 362 coldhead (brazed onto flange), and (Right) redesigned CHX intended for the "50K" coldhead (we wound up using it for the "70K" head testing). Note how the fin spacing on the original is very uneven.

Figure 11: The original CHX, after the fins were manually straightened with pieces of plastic shim to even out the slots.

Due to this and other design challenges, the "50K" coldhead was never built, though we finished nearly all the drawings for the parts. In part, we had hoped to use performance

results on the 70K coldhead to guide the final 50K design, but of course those results took much longer to acquire than anticipated.

Aftercooler design with CFD

During testing of the '226' coldhead (prior to the beginning of this project) we observed a hot spot on the aftercooler, opposite the water connections, that appeared very suddenly when the water flow dropped below ~6 liter/minute. CFD confirmed that this was due to a 'dead zone' in the flow, where the water just circulated locally and was not carried through to the outlet. This led us to employ CFD for the final design of the '362'-sized aftercooler. This turned out to be a good choice, because at this scale dead zones appear very readily, even at fairly vigorous flowrates. The CFD exercise helped us to optimize the placement and size of baffles to direct the flow and minimize dead zones. Figure 12 and Figure 13 show the solid model and some velocity plots from the final design:

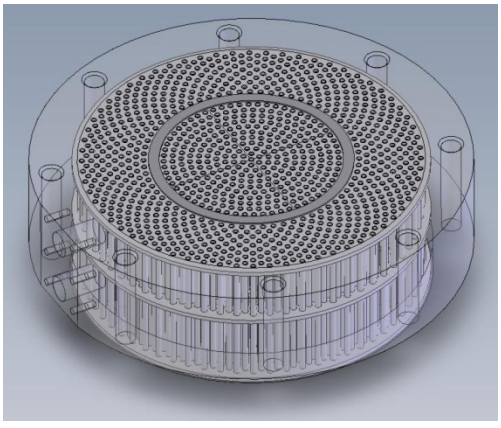

Figure 12: Solid model of ambient heat exchanger designed with the aid of CFD.

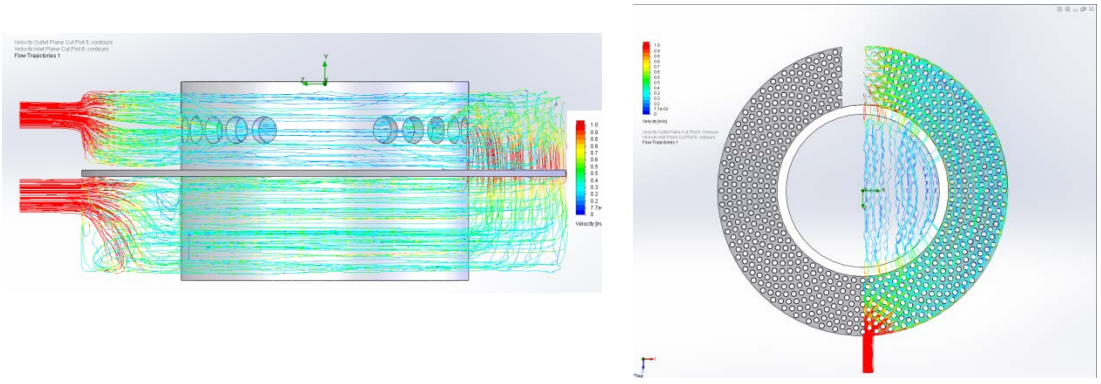

Figure 13: Flow trajectories with color-coded particle velocity, for 39 liter/minute total volume flow of water. Dark blue = 0 m/s, red = 1 m/s.

Cold-end flow management with CFD

One of the other risks of this large-scale coaxial 'pulse tube' coldhead is that as the working fluid is guided 'around the bend' in the CHX and the cold plenum, it will enter the cold flow straightener with too much momentum concentrated on either the center or the outer edge, and will not be sufficiently diffused when it enters the buffer tube. To

guard against that possibility, we enlisted the help of colleagues at Drexel University. Ph.D. candidate Dion Antao, and his advisor, professor Bahktier Farouk, modeled the entire coldhead between the aftercooler and the inertance tube in order to predict the effects of different cold-zone geometries. By modeling the entire coldhead, in 3D (or, a representative wedge of the rotationally symmetric construction) together with boundary conditions supplied by our 1-D thermoacoustic simulations, they were able to predict the velocity and temperature distributions in the coldhead at our "full power" operating point.

Originally, it seemed that the CFD model might yield an overall cooling power as well as the temperature and flow fields of interest. This would have given us a very meaningful reality check on the CFD, since modeling an acoustic cooler exercises the codes in regimes (such as conditionally turbulent oscillating flow) which have not been extensively validated. Given that the cooling power prediction in a CFD model is the average enthalpy flux, calculated from the difference of two much larger numbers (the maximum and the minimum) obtaining any precision in this number is a challenge; also, steady-state must be achieved, which means very long computation times. Ultimately, we did not insist on obtaining a cooling-power prediction to compare to data, though this remains important to us as a benchmark for establishing CFD as a truly reliable tool for acoustic cooler modeling.

In one case, Drexel modeled the plenum downstream of the CHX as empty; and in another iteration, the plenum was fitted with "turning vanes" designed to guide flow through the change of direction at the cold end. The spacing of the turning vanes partitioned the CHX slot area that discharges into the cold plenum into three tiers of roughly equal area, that were then guided to three concentric regions of the cold flow straightener of equal area. This was thought perhaps to prevent a radial maldistribution of flow going into the cold flow straightener. In both of Drexel's models, the flow and temperature maps did not suggest any mixing of hot and cold gas in the buffer tube. Figure 14 and Figure 15 shows some plots of the results without the turning vanes.

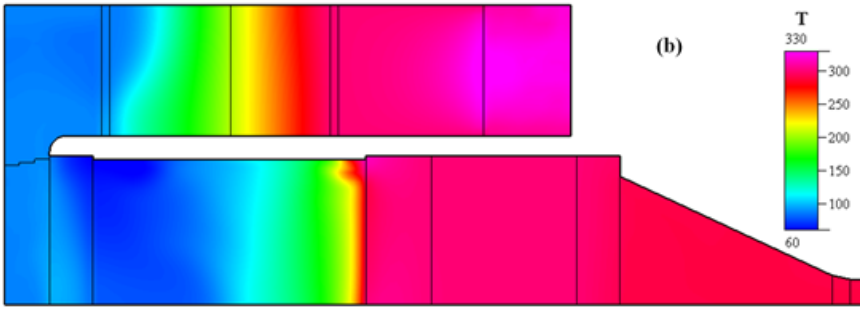

Figure 14: Plots of CFD results on our '362' coldfinger (actually, a side view of a 2.4 degree "pie slice" of the rotationally symmetric model) showing temperature at one extreme of the cycle. This is for the case with no 'turning vanes' in the cold-end plenum to guide the flow between the buffer tube and the cold heat exchanger.

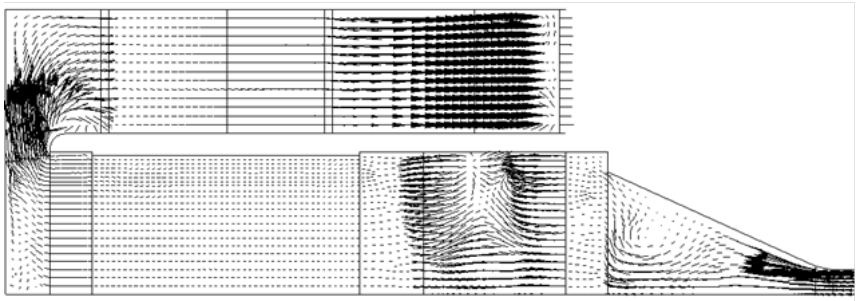

Figure 15: Another plot from the same CFD case as Figure 14, but showing velocity vectors instead of temperature.

As a result of our collaboration with Drexel, we had some confidence that if the coldhead were built as intended, there would not be an issue with flow distribution in the cold end despite its large size and relatively small aspect ratio. It's worth noting, however, that this effort was focused entirely on potential flow anomalies in the buffer tube, and assumes uniform flow into the ambient heat exchanger. Our experimental results eventually challenged this assumption.

Simulations with random fiber regenerator

One of the planned means of cost reduction was the replacement of the 1,000-or-so fine-mesh stainless-steel screens in the regenerator with 1/10th that number of ~1mm-thick annuli of random-fiber filter material. Compared to the exceedingly fine-mesh screen material in these coldheads (400 wires/inch) the random-fiber material is very inexpensive. We have already made this substitution in our '132' coldheads, which has resulted in the same or even better performance than we were getting with the fine stainless screens; so this seems like an obvious way to preserve performance while cutting costs. In our subsequent section on costing ("Low-cost manufacturing efforts") we discuss why this was not quite as dramatic a cost savings for the "362" coldheads. In this section, we focus on the performance penalty. For the 132 coldheads, the substitution of random fiber (using the random-fiber model included with Sage) into the simulations did not result in a predicted loss of cooling capacity or efficiency. In the "362" coldhead simulations, the increased power density seemed to result in a distinct penalty for using the random fiber. We spent a bit of time on these simulations, trying to optimize the fiber diameter and porosity for different segments of the regenerator (coarser wire size for the warmer end, progressing to finer toward the cold end) and trying to source material as close as possible to these optima. Nonetheless, it was a struggle to find a combination that approached the predicted performance of the woven screens[3].

[3] In theory, random fiber is in general not as good as woven screen for a regenerator because the pore size is not as uniform. However, in real materials it is easier to make a random fiber mat than a woven screen with fine fibers and high porosity, both of which are generally good characteristics, at least at moderate cryogenic temperatures. Fine fibers coupled with high porosity give a very small pore size with relatively low viscous pressure drop. Hence for many circumstances, random fiber may give comparable or better performance versus woven screens.

Figure 14 shows the prediction for our 50K coldhead, with screens versus random fiber. For the same pV power input, the cooling power is predicted to be 6% lower with the random fiber. This was not a big enough penalty to discourage us from pursuing this option; however, we did have a few options handy in case the actual random-fiber performance was disappointing. One was to use fine woven screens in just the very last part of the regenerator on the cold end. Another option would be to compress some of the random-fiber product to give it lower porosity (hence higher heat capacity), and place that in the cold end. The simulations do not appear to demand such measures, but they may not be capturing everything of importance.

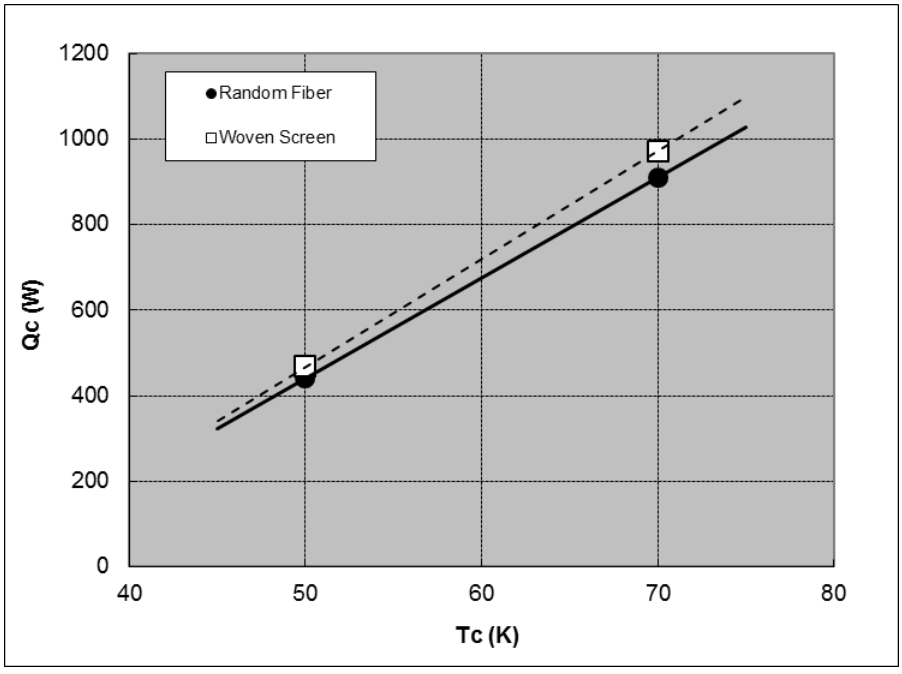

Figure 16: Predicted performance of "50K" coldhead with an optimized woven-screen regenerator versus optimized random fiber, for 15 kW *pV* input.

Coldhead assembly and testing

Assembly of flanged coldhead

At first, we did not procure the parts for a version of the 70K coldhead as shown in Figure 7, but instead, procured the parts for a version with a flange at the cold end. This would allow us to more easily make changes to the cold end, without having to remove the regenerator and buffer tube. Not only is this tedious, but risks damaging the regenerator screens, which are expensive and difficult to handle. Inserting and removing them multiple times also may ruin the crucial interference fit between the screens and the adjoining surfaces (the outside diameter of the buffer tube and the inside diameter of the regenerator housing). The interference fit is needed to prevent regenerator blowby, one of the most common causes of coldhead failure. The removable cold flange enables some changes without disturbing the regenerator packing; but achieving a helium leak-tight mechanical seal at cryogenic temperatures is not trivial. We have done this before in

much smaller coldheads, using indium O-rings. In our "132" coldhead, we built a version using CF vacuum-flanges and a copper gasket, and it worked very well. We attempted a similar construction here. However, at the "362" size, the forces are much greater compared to the stiffness of the standard flanges. Calculations suggested it could still work, but it did not have the same margin as at the smaller size.

The first test coldhead featured a welded aftercooler, in contrast to the brazed aftercoolers in our "241"-size coldheads developed during Phase II. This significantly decreases the manufacturing cost (see "Low-cost manufacturing efforts," further on in this report). The welded construction also makes fixing leaks much easier, and several were found in this first article. The fine details of the weld joints and the welding process was one of the major design efforts in this project. Like the '241' coldheads, the buffer tube is made of Garolite XX and has the flow straighteners glued in place to prevent any possible blowby into the buffer tube. Figure 17 shows the new aftercooler and the buffer tube/flow straightener assembly inserted into it.

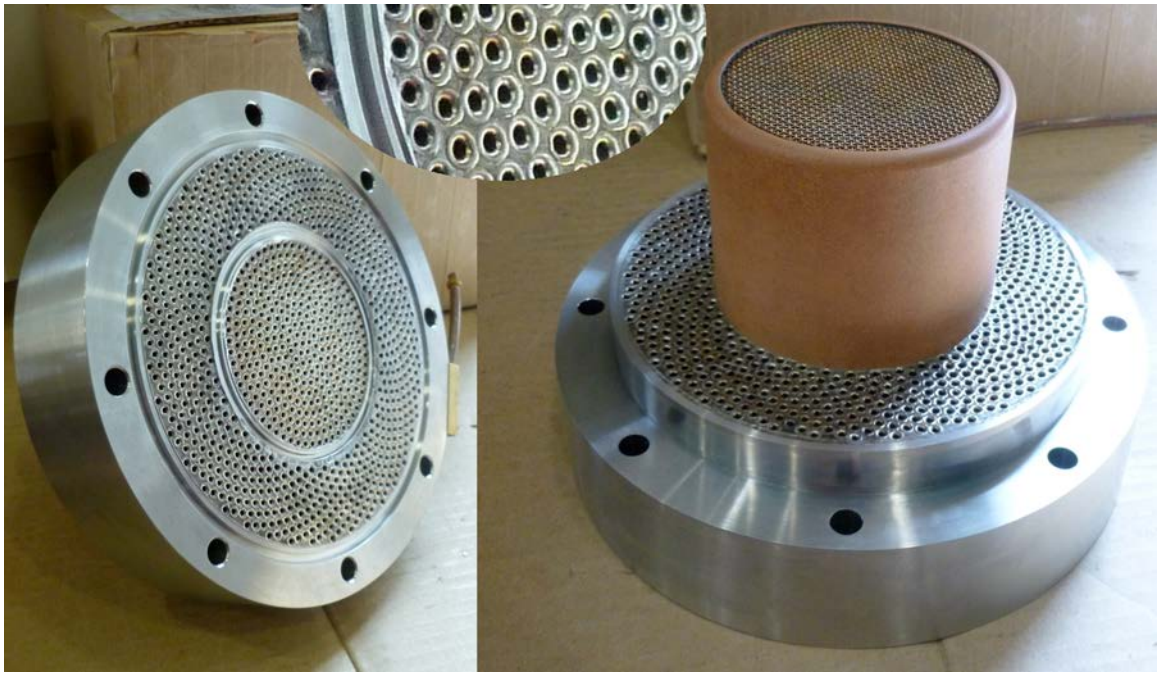

Figure 17: Welded aftercooler, w/ buffer tube assembly and detail of tube weld joints.

Figure 18 shows additional views of the coldhead going together for the first time.

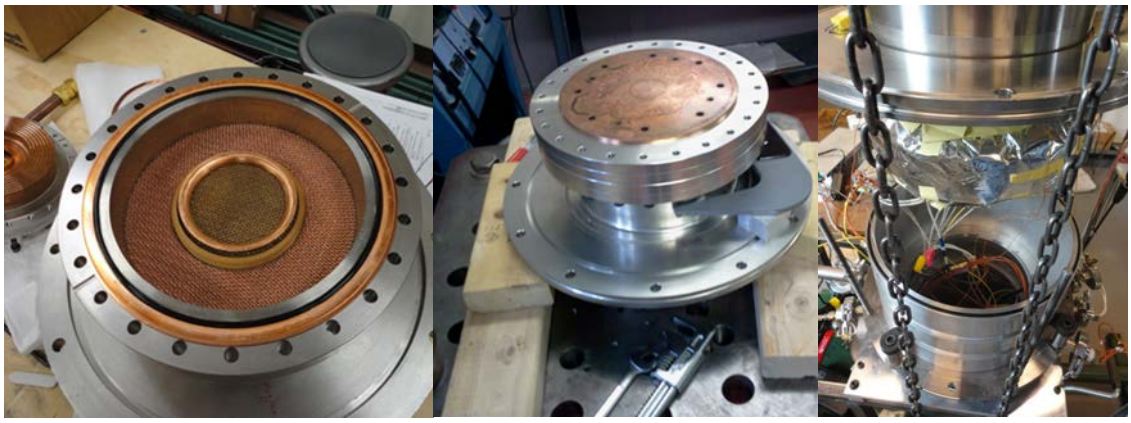

Figure 18: (left) Cold-flanged head with cold cap off; (middle) after bolting it on. Assembly is under pressure, and the micrometer is being used to measure distension of pressure vessel. (right) The coldfinger is wrapped in MLI, instrumented, and being lowered into the vacuum vessel.

When the coldhead was completely together and instrumented, it was attached to the 2S362W PWG using the 2-m-long rigid transfer line, and an external inertance tube, uncoiled, approximating the coiled version shown in Figure 8.). The entire experimental assembly is shown in Figure 19.

Figure 20 shows the first cooldown of the 2S362K-FAR, at low power (~7kWe input out of a possible ~20 kWe). One reason for running at low power was to reduce the thermal stresses on the coldhead by keeping things closer to a quasi-equilibrium. Even at this slow cooldown rate, the cold-end flange began leaking, and the vacuum degraded significantly. Only when the temperature approached 50K and the cooling rate slowed down did the vacuum recover; it stayed at or below 100 mTorr for the rest of the run. Generally, we consider ≤10 mTorr to be a "good" vacuum, meaning that convection in the vacuum can has a negligible effect on the measured capacity of the coldhead. At this scale, the convection losses are less important than in our smaller coldheads, due to the lower surface/volume ratio. Nonetheless, we strove for lower vacuum in subsequent runs.

We experimented with frequencies near 50 Hz (our nominal target) and got our best low-power heat-load results at 49 Hz, 5kWe input, as shown in Figure 21. A very simple extrapolation says that the gross cooling power of the coldhead ought to scale with input power; and that the heat leak (primarily conduction down the regenerator wall) will stay relatively constant with input power, which allows us to roughly estimate the ideal performance of the coldhead at higher input power. To extrapolate properly, we have to know the magnitude of the 'heat leak,' or the amplitude-independent parasitic heat load (mostly conduction through the regenerator shell). There are several ways to quantify this. Two of the easiest are to (1) shut the power off to the cryocooler and watch how quickly the coldtip warms up (without heat load), and from the amount of stainless steel and copper in the cold end, estimate the heat capacity (which will tell you how much heat must be flowing into the cold end to warm it up), and (2) to repeat the same test with some applied heat load, and compare the warmup rates with and without heat load.

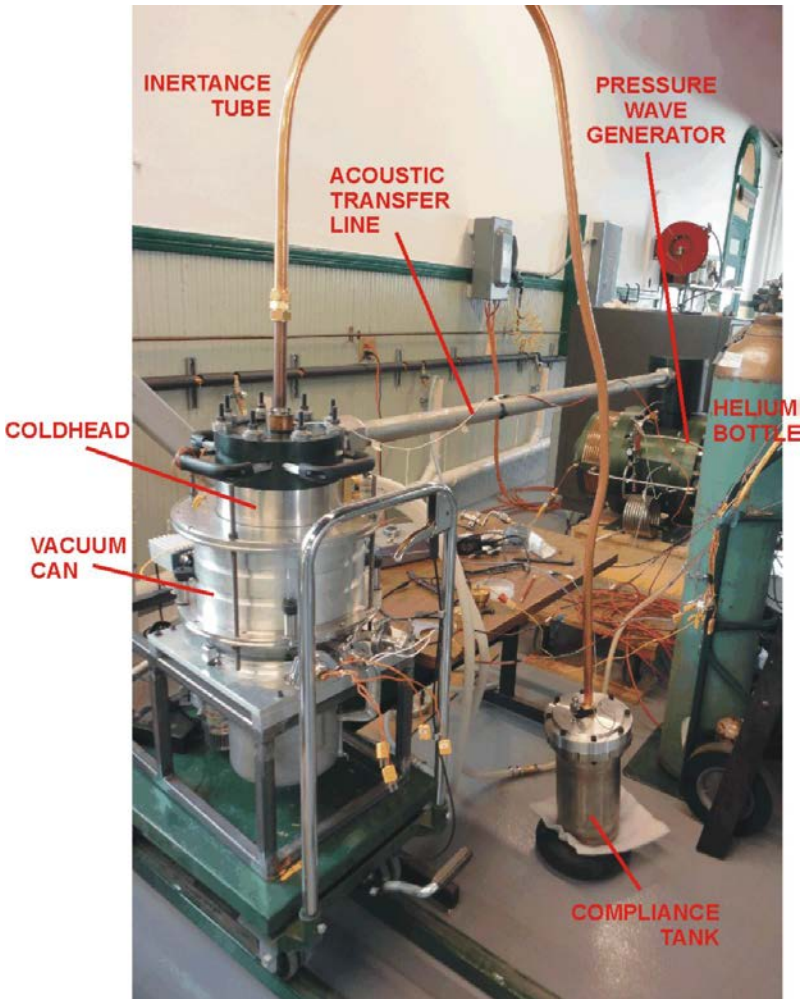

Figure 19: Setup of 2S362K-FAR cryocooler for first cooldown.

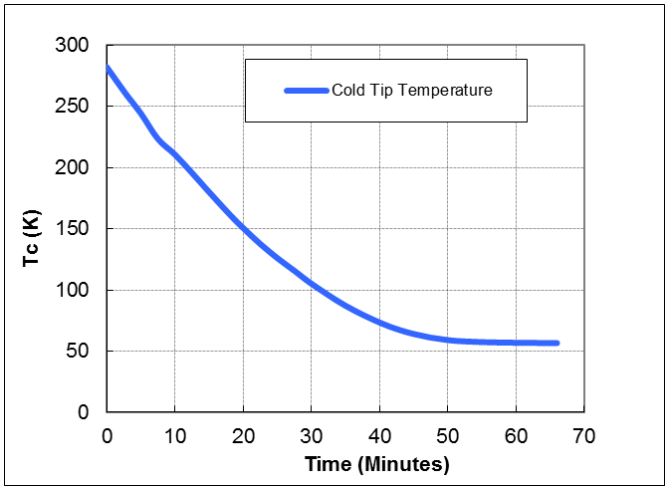

Figure 20: First cooldown of the 2S362K-FAR, with 5 kWe input.

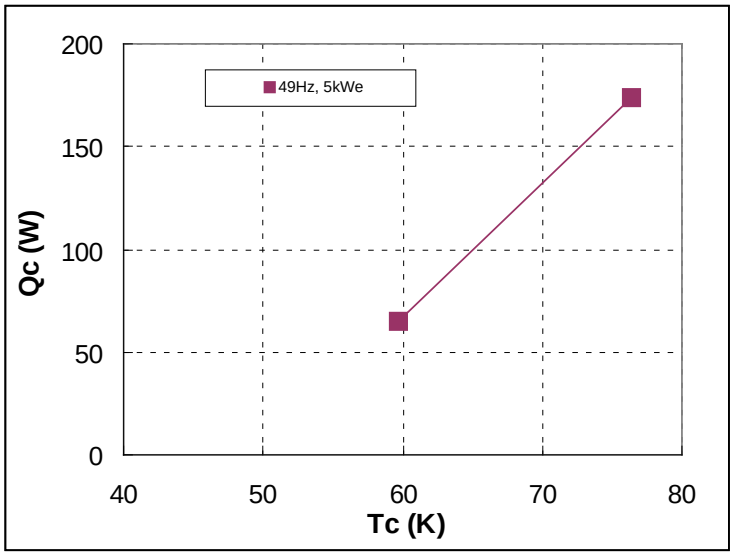

Figure 21: Two-point 'load curve' at 49 Hz, 5 kWe input.

Both methods indicate that the heat leak at 77K is around 100 watts. Thus, the "gross" cooling power at 77K (and 49 Hz, 5kWe input) is 174+100=274 watts. At full power, or 20 kWe input, you would expect the gross cooling power to be 274×4=1096 watts. The heat leak, however, barring amplitude-driven streaming or other pathology, remains the same; so the expected net cooling power at 77K, 20kWe input is about 1000 watts. That's near what the simulations predict, so this suggests that the fundamentals of the coldhead are correct.

However, other measurements done during this run suggest that success will not be so simple. Figure 22 shows the cooling capacity at 77K for 5 kWe and 10 kWe input; the capacity hardly increases, even when the input power is doubled.

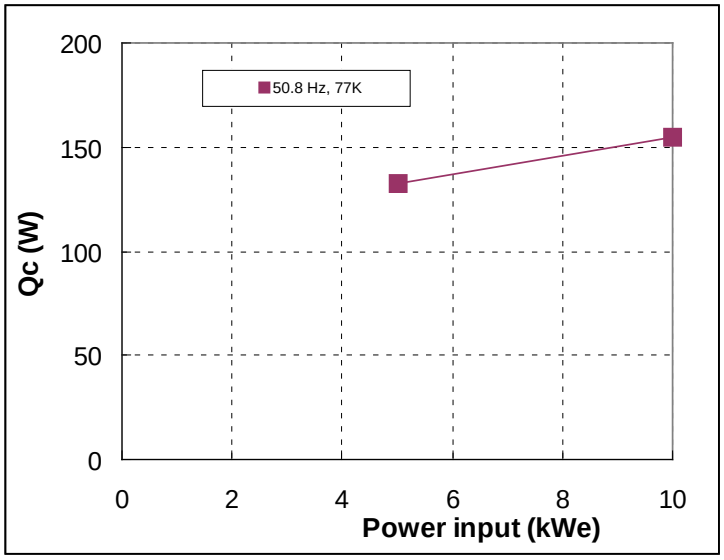

Figure 22: Net cooling power at 77K, as a function of input power to the PWG.

This is our first indication that the coldhead has a serious flaw, most likely a flow anomaly that gets more pronounced at higher amplitudes.

After this first set of tests, we were not able to get a good vacuum again in the flanged coldhead. The metal-on-metal seal is particularly unforgiving if the parts warp or distort in any way, since the metal won't fill gaps. The assembly turned out to be very susceptible to creep from thermal cycling, so although we got a decent (not excellent) vacuum on our first run, once everything reached steady state (and the cold end was more-or-less uniform in temperature), it was not repeatable once the coldhead was brought back to room temperature and cooled again.

At this juncture, with the benefit of hindsight, we should have abandoned the cold-flanged head. Instead, we attempted a number of ways to get the cold end to seal, including first a Mylar and then a nickel gasket in place of the original copper. Copper has a higher coefficient of thermal expansion (or contraction) than the nearby stainless steel; hence we theorized that the original copper gasket was shrinking in its groove, pulling away from the knife-edge features impinging on it. A metal with a more similar thermal expansion might not, we supposed. However, it made little difference in practice.

While experimenting with various means of achieving a tight seal at the cold end of the flanged head, we began procuring parts for a version with a fully brazed cold end, using the less costly CHX we had designed for future builds (with fewer, wider slots) as shown previously in Figure 10. These parts were received before we were able to successfully maintain a helium-tight seal in the flanged coldhead; so we shelved it and moved on to the brazed version.

Assembly of brazed version

We used many of the same parts in the buildup of the brazed version, including the aftercooler and many of the regenerator screens (those in the best condition after removal from the flanged head). Figure 23 shows the coldhead components on the bench before assembly, and the final assembly. The buffer tube is threaded into the aftercooler, and the screens are loaded on the buffer tube. The regenerator housing/coldtip brazement is then lowered down over the regenerator, with threaded rods through the aftercooler and junction block into the RGR housing to align everything. Working several of the nuts down the threaded rods, until they compress the washers, pushes the RGR vessel over the regenerator screens, until the vessel flange meets the mating surface on the aftercooler. Thus the cold end of the buffer tube is inserted into the cold heat-exchanger plenum "blind"; we are counting on the alignment provided by the threaded rods to ensure that the parts are centered when they go together. Also, we now cannot remove a flange from the cold end and examine the fit of the RGR screens, nor modify the cold-end configuration (e.g. remove turning vanes) without disturbing the regenerator. It does seem, however, that we can take the RGR vessel off without dislodging the regenerator

screens; they tend to stay on the buffer tube, which is threaded into the aftercooler. This makes changing the regenerator configuration a bit easier and lower-risk than if the regenerator screens had to be pulled out by hand bit-by-bit.

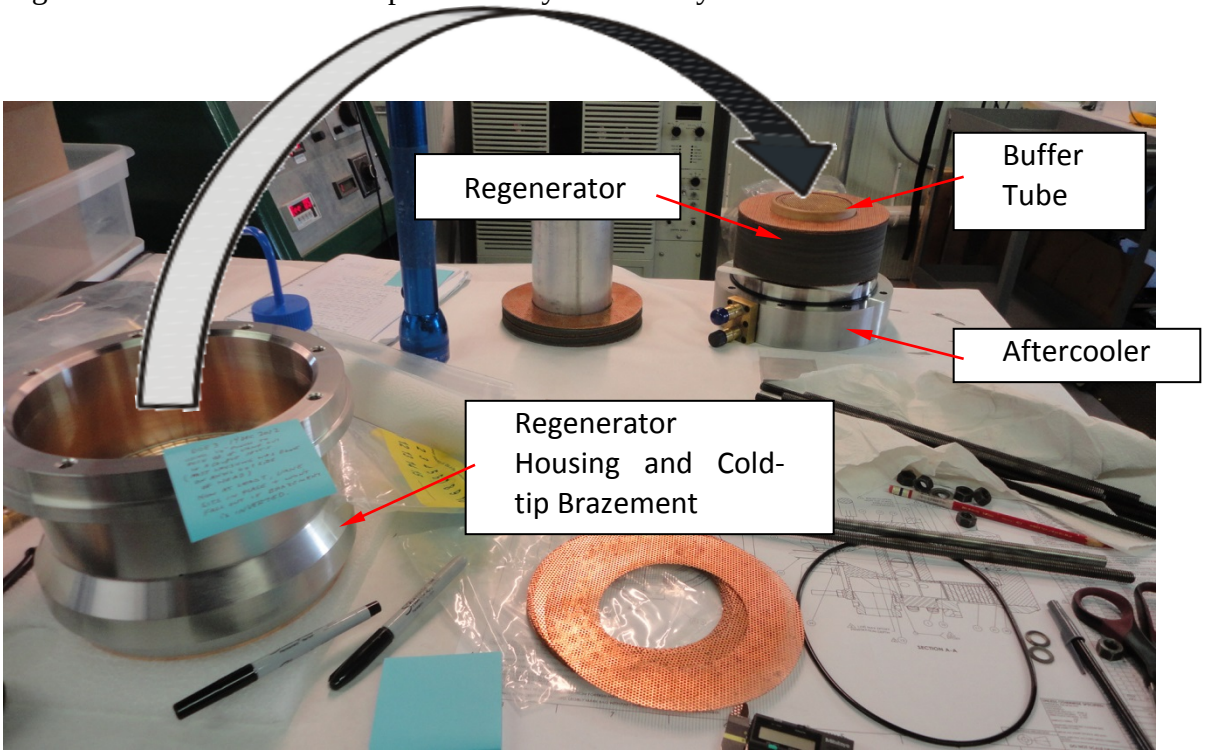

Figure 23: Brazed version of "70K" coldhead going together on the bench.

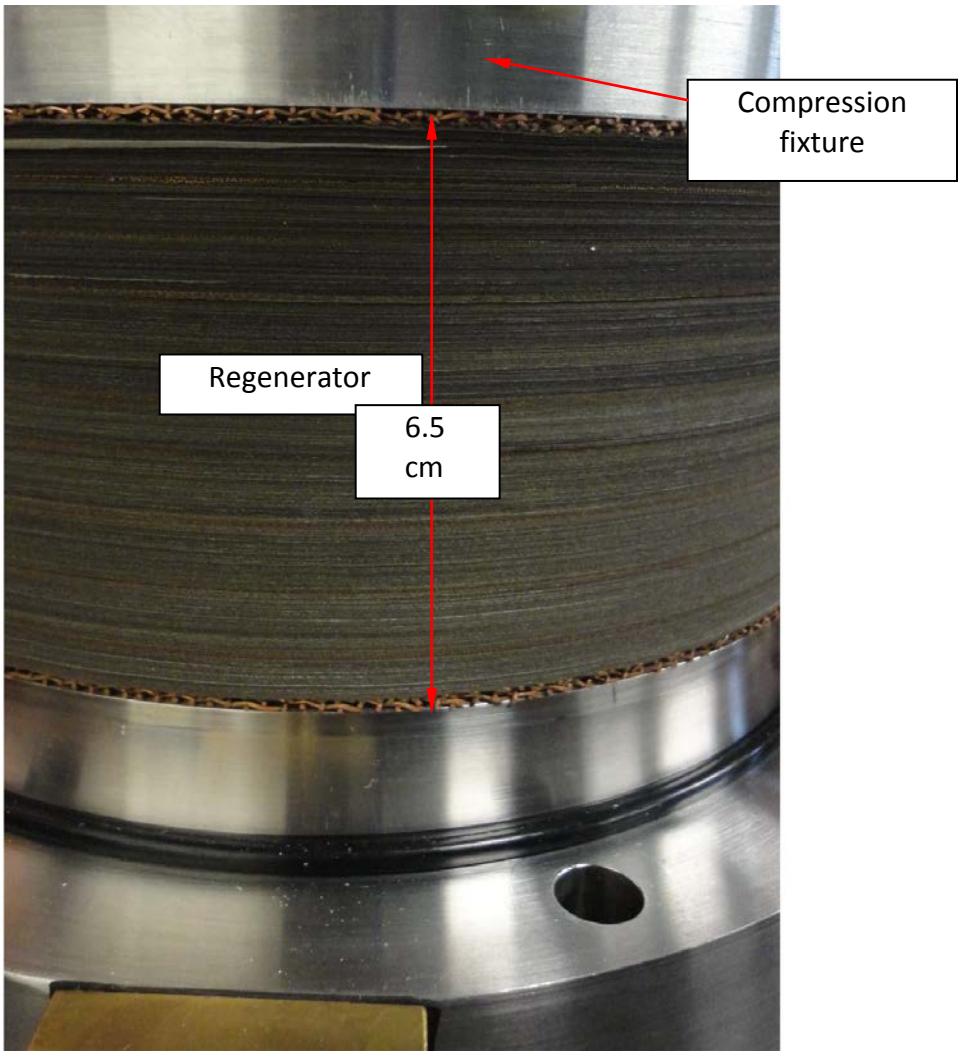

Figure 24: The regenerator, loaded in place, before the compression fixture is removed and the brazed coldhead vessel is lowered on. The regenerator screens are mostly fine-mesh stainless steel, but one can see the coarse copper screens on the top and bottom, and streaks of orange in the body of the regenerator every ~0.7cm are the intermittent fine copper screens..

Figure 24 shows the regenerator stack from the side. This version has intermittent copper screens to aid in locally isothermalizing the regenerator; the next version will use more robust perforated copper rings for more aggressive isothermalizing.

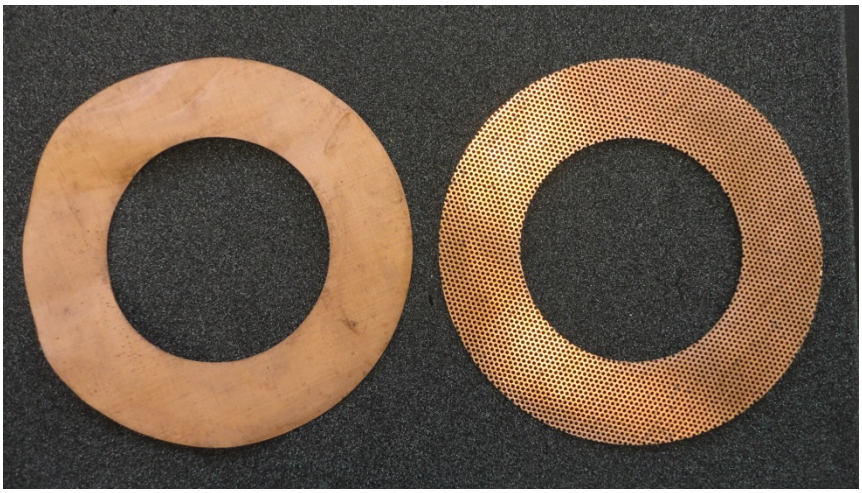

Figure 25: Fine-mesh copper screen (L), perforated copper ring (R).

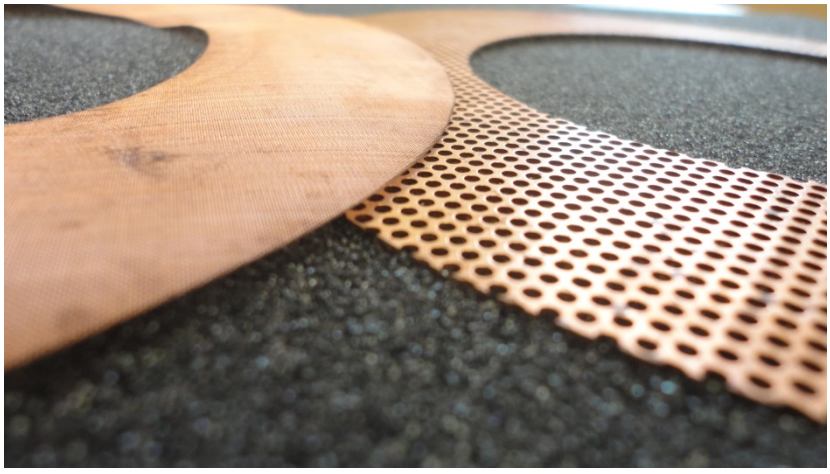

Figure 26: Closeup of fine copper screen (L) vs. perforated ring (R). The ring has much greater thermal mass, but also less open flow area.

Figure 25 and Figure 26 show the two thermal equalizers side-by-side. The choice of one versus the other is a matter of balancing thermal mass against disruption of the flow in the regenerator. The fine copper screens are almost invisible to the flow, but of course they have relatively little thermal mass compared to the perforated rings. The perforated rings, on the other hand, have a much lower percent open area and overall occupy a greater percentage of the regenerator volume. Hence, they might interfere with the regenerator's core function more than the copper screens, even as they maintain more uniform temperature.

Figure 27 shows the full system assembled and ready for testing. With the coldhead inside the vacuum can, the system looks about the same as with the cold-flanged head (except that we have tidied up the wires, tubes, and instruments a bit.)

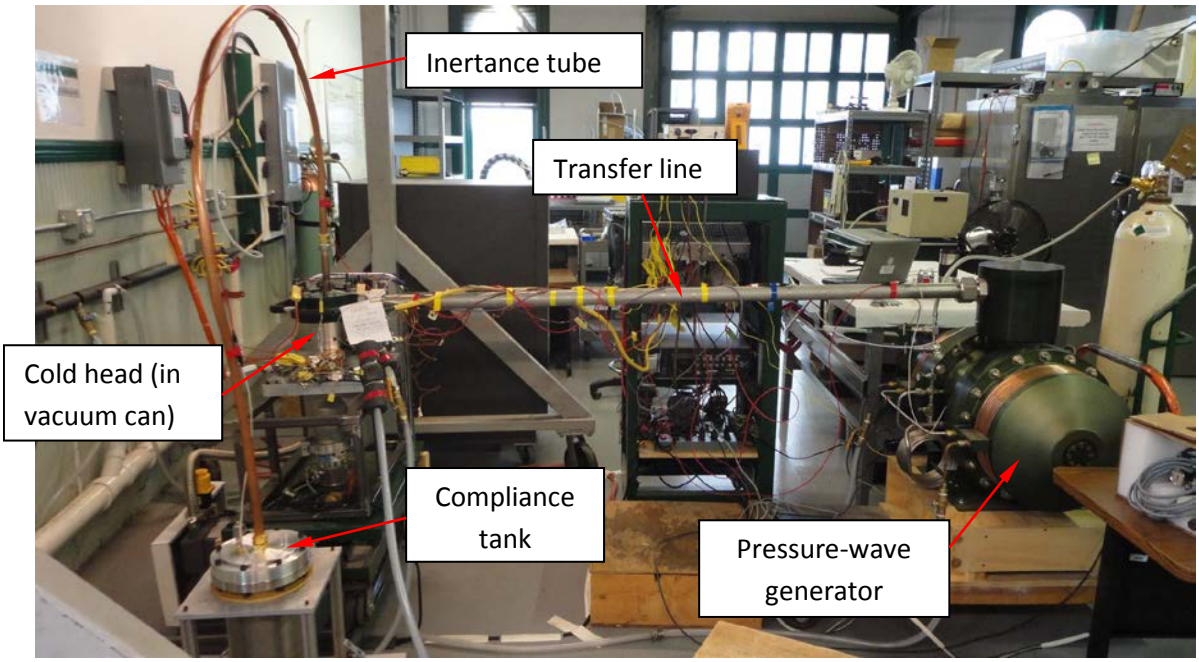

Figure 27: Assembled 2S362K test system, with brazed regenerator vessel/coldtip.

Thanks to the brazed joint at the cold end, we had no trouble with helium leaking into the vacuum can from the coldhead; and we were able to do a much more extensive map of the system's performance as a function of input power and coldtip temperature, as shown in Figure 28. With these data, a distinct trend is apparent. The graph shows cooling power versus input power curves at 70K, 80K, and 90K. For a completely healthy acoustic cryocooler, these would be fairly straight lines. Instead, as power increases, these curves bend over. The effect is more pronounced at the lower temperatures, particularly at 70K, where the cooling power almost flattens above 4 kWe input.

Of the known pathologies that can afflict acoustic cryocoolers, these data most strongly suggest streaming within the regenerator, that is, a convection cell that feeds on and exacerbates differences in temperature that exist in the planes perpendicular to the axis of acoustic power flow. The observed performance degradation in our system shows sudden onset with amplitude (at least, in the at 70K data) and significant temperature sensitivity, which are markers for regenerator streaming [5]:

> *"As a regenerator is scaled to higher power or operated at lower temperatures, the thermal and hydrodynamic communication transverse to the acoustic axis decreases, allowing for the possibility of an internal acoustic streaming instability…"* J. H. So and G. W. Swift, from [5]

This is also echoed in the temperature distribution around the regenerator midpoint, which becomes progressively less uniform as the input power increases, and as the cold-tip temperature decreases.

This characteristic is distinct from what one might expect from a flow disturbance in the buffer tube—in that case, the lost cooling power would be a weak function of coldtip

temperature, and a stronger function of acoustic amplitude. As coldtip temperature increases, for instance, the pressure wave amplitude in the buffer tube is generally higher for the same input power. Thus, we might expect that if a flow disturbance in the buffer tube were to blame, the disturbance would be at least as bad if not worse at the higher coldtip temperatures. This would be only slightly offset by the smaller thermal gradient (the difference between ~310K–70K vs. ~310K–80K or 310K–90K).

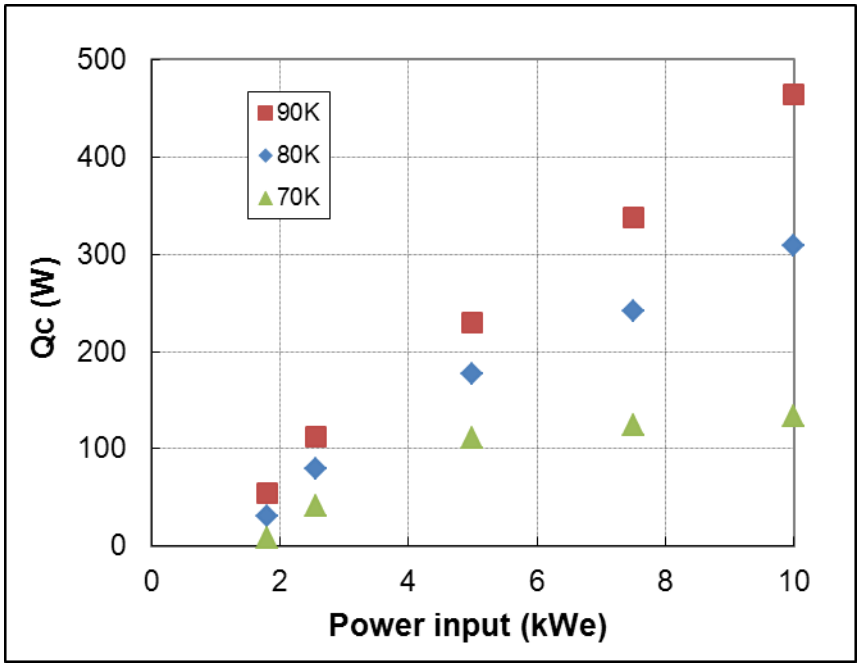

Figure 28: Load map of the configuration in Figure 27, all at 51Hz and 28 bara charge pressure.

Indeed, in other instances when we have encountered nonuniform flow in the buffer tube of a coldhead, the load lines tend to be more parallel, just offset vertically from where one might expect (the result of a convection loss that is only weakly dependent on temperature). Regenerator streaming, on the other hand, is observed to have exactly this behavior—a strong dependence on amplitude *and* temperature.

At the time these data were initially collected, we had one suspected cause, and cure, for the observed pathology. In the initial build, we used the weaker of the two "isothermalizers" (the fine copper screens). We repacked the regenerator with the perforated coppers (as shown in the right side of Figure 1, which are intrinsically much stronger at equalizing lateral temperature differences—and got almost *exactly* the same results. This suggests that (1) the main problem was not (merely) lack of lateral conductivity, and (2) the problem was also not something particular to how the regenerator was packed. For instance, we might have guessed that the main culprit was flow bypassing the regenerator due to unintended gaps between the regenerator elements and the regenerator I.D. (or the buffer tube O.D.). Buffer-tube flow disturbances and regenerator bypass flow are the two most common causes of poor 'pulse-tube' coldhead

performance, at least at smaller scales. In this case, it seems like something else—perhaps the regenerator streaming mentioned above. In any event, we have to find another means to diagnose and repair the problem.

One aspect of the cryocooler construction that we anticipated might be an issue is the side entry of the transfer line into the coldhead. The side entry is very convenient, but it does introduce an obvious source of flow asymmetry that might initiate convection in the regenerator. One possible way to observe this is by the temperature distribution around the midpoint of the regenerator O.D. If everything is ideal, the regenerator midpoint is about halfway between the coldtip temperature and the reject temperature, and uniform all the way around. If there is a circulating flow in the regenerator, it could cause a bias in the temperature gradient. In particular, we can imagine that when flow is coming *out* of the transfer line, its momentum causes it to impinge more on the side of the aftercooler opposite the entry point; whereas when the flow is going *into* the transfer line, the side exit does not exert much of an influence on the flow distribution. This could induce a pattern of flow down the far side and up the near side, relative to the transfer line entry. This would tend to raise the temperature at the midpoint on the far side (as helium is flowing down from warm to cold) and lower the temperature on the near side (as cold gas is pushed up).

Figure 29 shows how thermocouples are placed in four locations around the regenerator circumference, to approximate the temperature distribution at the midpoint. One way to present or visualize the temperature around the regenerator is as a virtual "frost line." That is, if the coldhead is run in open air, without a vacuum can or MLI wrap, frost will form around the cold portions of the head, ending at a line where the temperature drops below 0°C. Ideally, this line would be level all the way around the coldhead; but if there is some kind of flow imbalance or pathology, the 'frost line' will be distorted as a result. Figure 30 shows how this might look.

The temperature around the regenerator circumference can be presented in a similar fashion, as a virtual "frost line," around a circle with the height representing decreasing temperature. Figure 31 shows the results corresponding to the 70K data points of Figure 28. The height of the plot corresponds to the magnitude of the temperature in Celsius (the temperatures are all negative), with the shape of the plot resulting from a smooth connection of the four temperatures. Despite the paucity of temperature data, the suggested shape of the "frost lines" is very suggestive of the phenomenon we think might be happening in the regenerator as a result of the transfer tube's side entry into the plenum above the aftercooler.

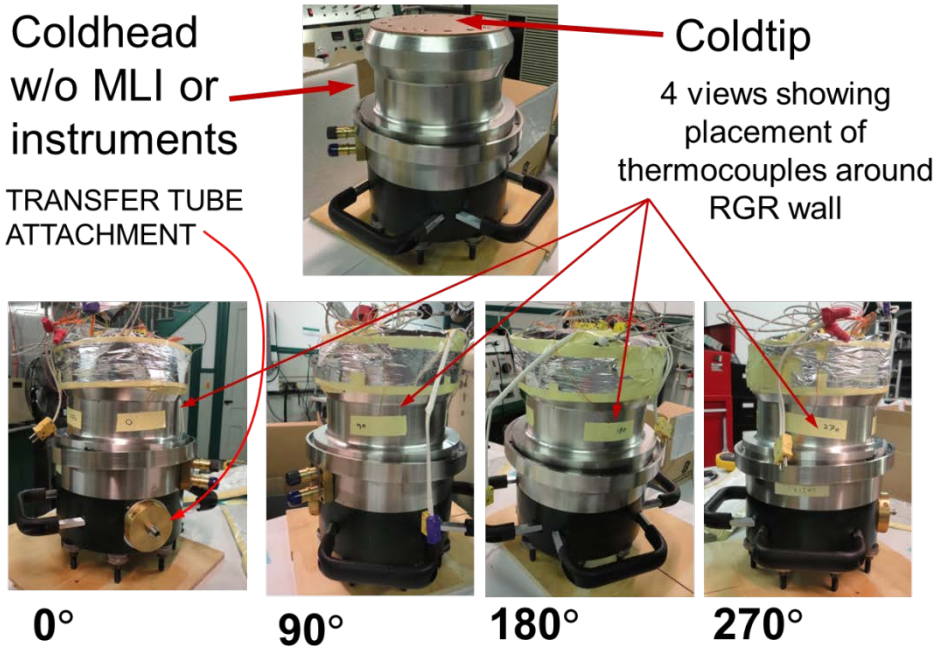

Figure 29: Views of the brazed coldhead in various rotations, showing the placement of thermocouples around the circumference of the regenerator vessel.

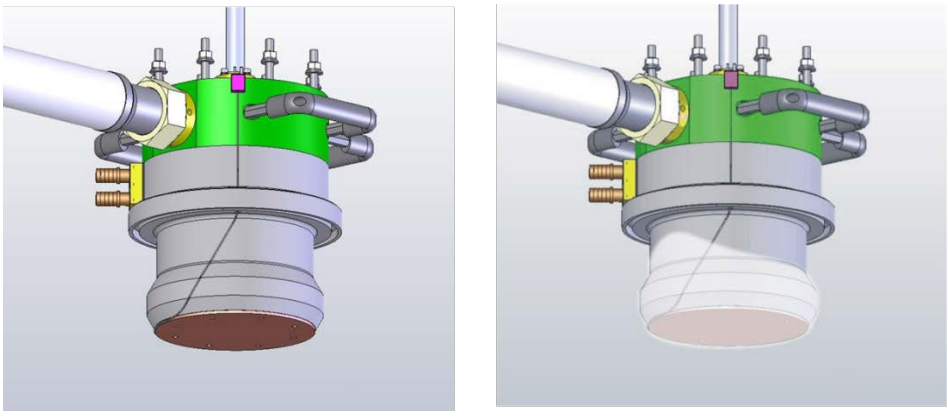

Figure 30: A solid model of the coldhead, with transfer line; the right side showing how a distorted frost line might look if there is a circulating flow in the regenerator caused by the transfer line entry.

This is hardly a smoking gun, however. In many other tests of large coldheads, we have seen big swings in temperature around the circumference of a regenerator, and these big swings are not always correlated with performance. The alignment of the 'frost line' with the transfer tube could be coincidental. To really make the case that the side entry of the transfer line is skewing the temperatures, we rotated all parts of the coldhead assembly relative to the transfer line by 90 degrees, except the junction block where the transfer line attaches. The two assemblies are shown pictured side-by-side in Figure 32. Figure 33 shows the "frost line" plots at 10 kWe input, with the cold tip temperature at 70K and the reject at 298K, before and after rotation.

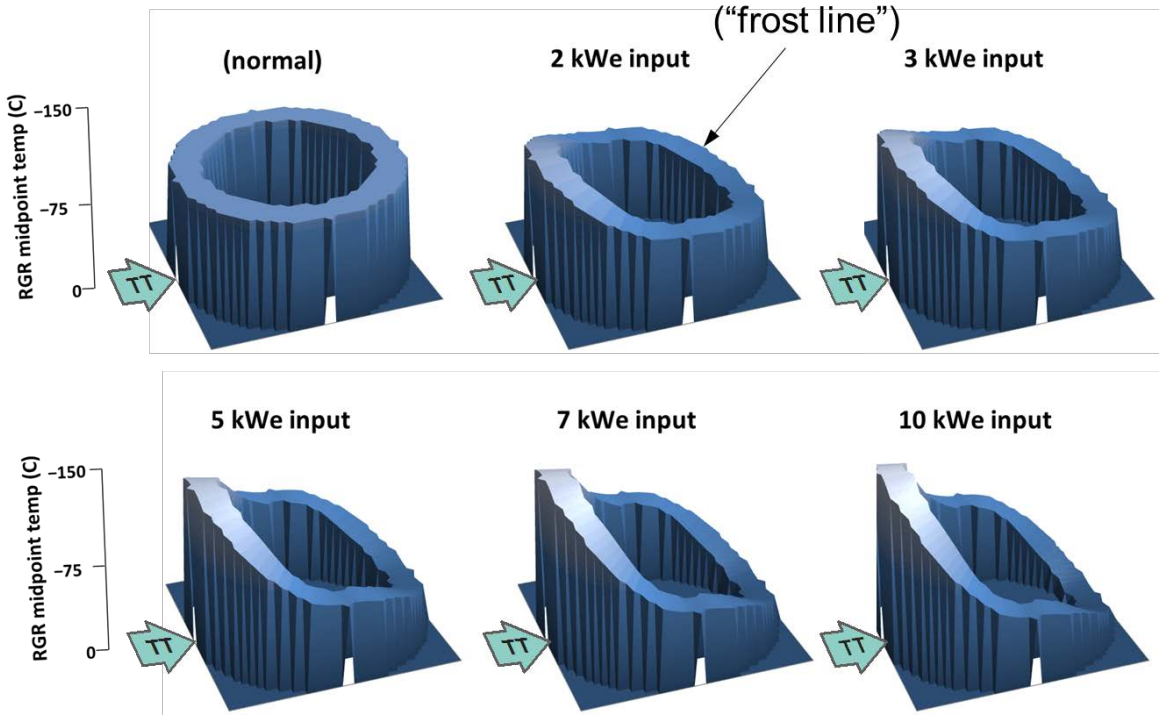

Figure 31: Virtual "frost line" plots of the temperature around the circumference of the regenerator, for the 70K data shown in Figure 28. The "TT" arrow shows the location of the transfer tube, where acoustic power comes into the coldhead.

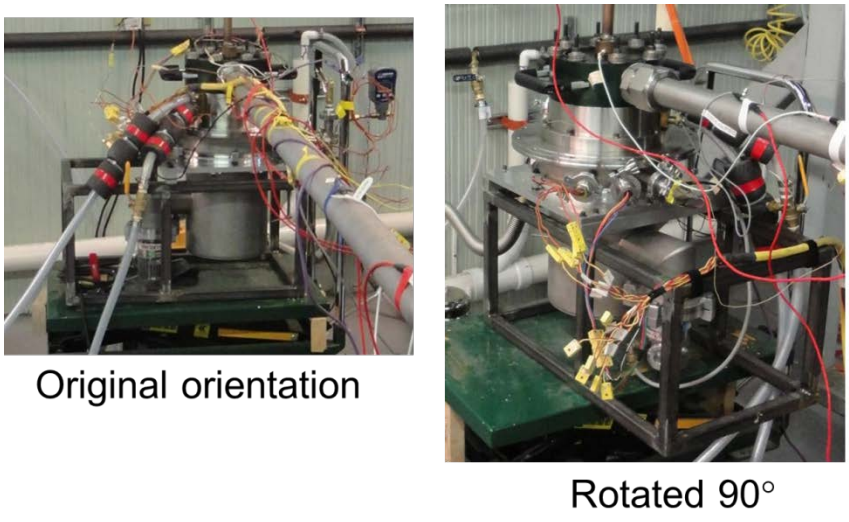

Figure 32: The coldhead assembly before and after being rotated 90 degrees relative to the transfer tube attachment. Note how the cooling water lines move from the left side of the transfer tube to the right side. Everything below the green junction block with the handles on it is moved together as a unit 90 degrees counterclockwise, looking down on the assembly.

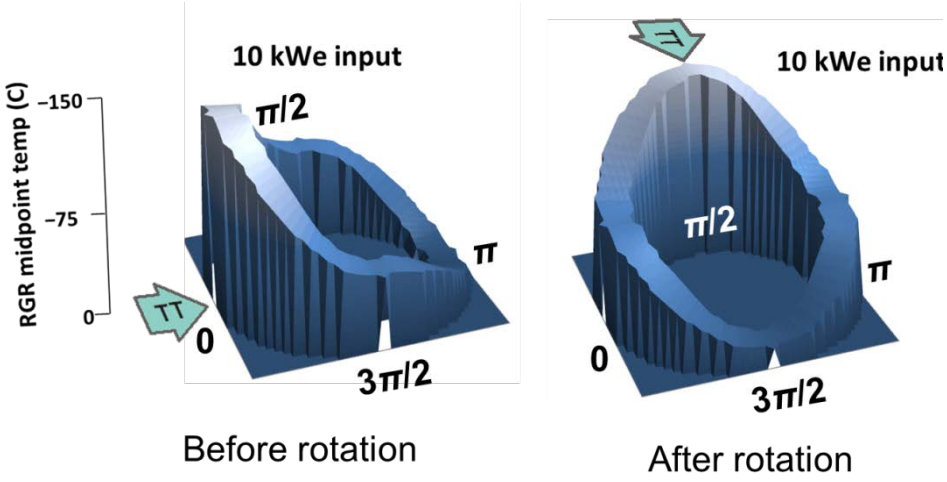

Figure 33: "Frost Line" plots of the temperature around the regenerator midpoint before and after the coldhead was rotated 90 degrees relative to the transfer tube location.

The skewing of the temperature around the regenerator stays aligned with the transfer tube, and does not rotate with the coldhead (note that the thermocouples stay attached in their original locations on the regenerator at it is rotated, and they are identified with their angular locations on the regenerator). This provides very strong evidence that it is the side entry of the transfer tube, and the resulting asymmetric flow disturbance, that causes the skewing of the temperatures. If the temperature profile is indeed a symptom of regenerator streaming, then we may have identified one factor in the poor performance.

Understanding in detail how the side entry might disrupt the flow is more challenging. Other than the qualitative argument given earlier (on page 34) we don't have criteria to drive a redesign. We can certainly suppose that the volume in the junction block is insufficient to diffuse the flow coming from the transfer tube, but no good sense of how much bigger it ought to be. We turned to CFD, briefly, to give us a little guidance in this regard. Figure 34 shows a CFD flow map of the original design, which does indeed predict a very uneven distribution of flow through the regenerator. We intended to use further CFD simulations to verify that a given increase in the vertical dimension of the plenum would evenly distribute the flow, but time constraints forced us to take a guess. We chose to approximately double the plenum volume with a simple ring inserted between the original junction block and the aftercooler. Figure 35 shows the coldhead with the ring inserted; the ring is much shorter than the junction block, but the junction block is conical inside (see Figure 7).

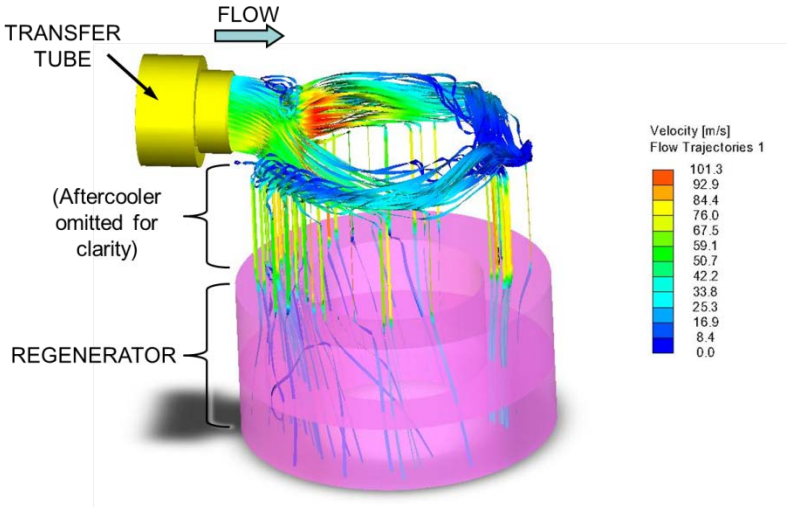

Figure 34: CFD flow map at peak positive flow from transfer tube, showing how the predicted flow is very uneven in the regenerator.

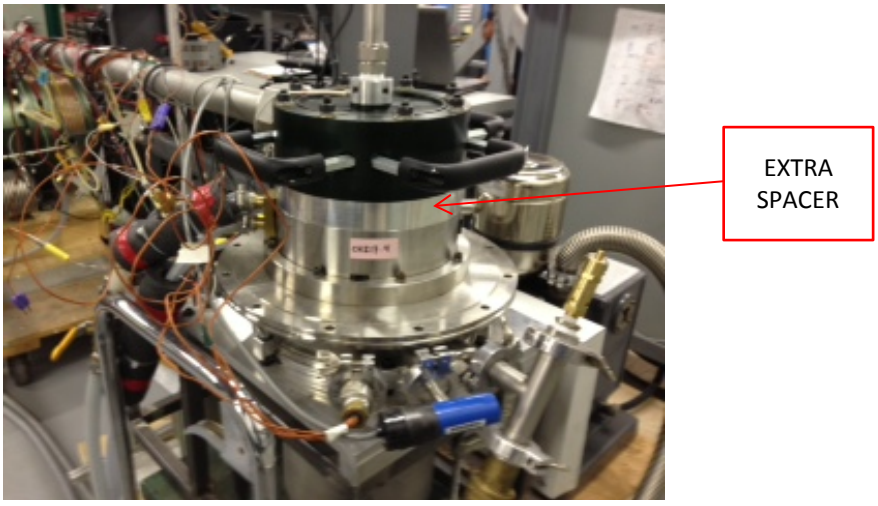

Figure 35: Experimental setup very much like the right side of Figure 32, but with an extra spacer ring between the junction block (where the transfer tube connects) and the aftercooler, to help diffuse the momentum of the incoming flow from the transfer tube.

Figure 36 shows the results with the extra spacer ring, compared to original build, without the spacer ring. The improvement is dramatic, especially at 70K. The cooling power at 70K is more than doubled at 10 kWe input, while being essentially the same at very low power. This suggests that the extra "breathing space" created by adding the spacer ring has significantly mitigated whatever amplitude-dependent pathology is affecting the coldhead.

Oddly, perhaps (but in keeping with our previous observations about regenerator wall temperatures) the dramatic improvement in 70K performance at 10 kWe input was not strongly reflected in the temperature distribution around the regenerator. Before insertion of the spacer ring, the maximum delta between the four measured temperatures at this operating point was typically 132K; after insertion, 120K. While certainly an

improvement, it's not exactly proportional to the gain made in cooling power. Perhaps it indicates there is still some regenerator streaming, that can be eliminated with even better flow management at the transfer tube entrance.

While the improvement seen with the spacer ring is a significant victory, there are still many more gains to be expected from the usual sorts of optimizations applicable to a 'pulse-tube' cryocooler, most notably from adjustments to the inertance tube length and the transfer-tube length. The inertance length (and perhaps even diameter) can be modified to optimize the cycle phasing in the coldhead, and the transfer-line length helps match the 'compressor,' or pressure-wave generator, to the coldhead for maximum power delivery. Neither of those lengths is likely to be optimal in a first build; while the simulations are good for finding a good starting place, the actual impedance of the coldhead and the cycle phasing are only approximated by the codes. Experiments are usually needed to refine these values. Therefore, we can reasonably expect that at least modest increases in efficiency can be added to the substantial gains already realized with the extra aftercooler plenum volume.

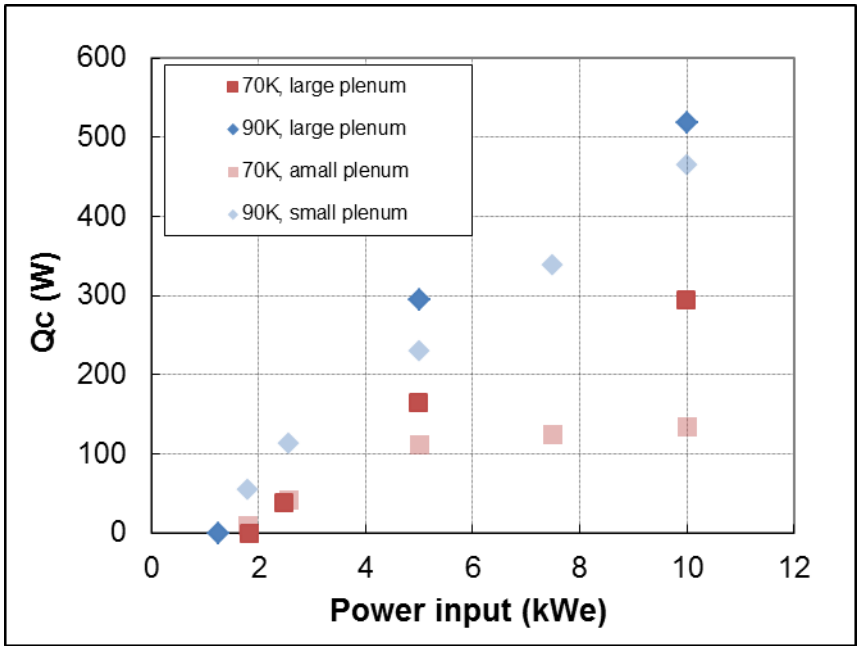

Figure 36: Cooling power for the system shown in Figure 35, compared with that of Figure 27 (that is, with and without the extra spacer ring in the coldhead).

Indeed, subsequent tests at higher input power showed that the highest cooling power at 80K occurred not at resonance (approximately 49Hz) but at 51 Hz, in spite of the higher current draw. This means the inertance tube is probably too short, so reducing the wavelength (by increasing the frequency) helps the cycle phasing. We were just beginning to explore inertance-tube changes when we had a load-plate heater fail. The data we were able to collect are those shown in Figure 1, which indicate that even without any further improvements, just higher power, we would come very close to

reaching our nominal goal of 1000W at 80K for 20 kWe input. Since further improvements were likely, with more plenum volume or other flow management at the transfer-tube entrance, and better impedance matching between the PWG and coldhead, we were very encouraged. Unfortunately, we could not implement these improvements, due to time, space, and budget constraints.

A burned-out load-plate heater would not normally be a major issue, but we had another big system test in the queue (a 2S362K oxygen liquefier for the Navy) and there was no time to make repairs to the DOE system. In addition, the space and much of the equipment were needed for testing the Navy system. At this point (March of 2014) we were already well past the "period of performance" for the DOE grant, and we were essentially working on the project on indefinite unfunded extension. The belief was that good, positive results would prompt Chart, Inc. to commit development dollars toward commercializing the DOE system. When it was apparent that we would have to stop testing the DOE system for repairs, we had to make the difficult decision to mothball it and focus on the Navy system and our other work in progress.

Initially, we thought perhaps we would revive the DOE system, as a way of demonstrating basic feasibility of the technology at the larger scale to our parent company. However, being part of a company that makes cryogenic infrastructure has taught us that the coldfinger approach might not be very appealing for the applications of interest to Chart, such as zero-boiloff storage or natural-gas liquefaction; and even now (in 2016) a robust HTS market has yet to emerge.

Hence, our decision to formally end the present investigation and file this report.

Flexible transfer line design and testing

Due to the coldhead challenges, the flexible transfer line work fell to a lower priority. The main effort in this regard was prototype design, based on lessons learned in Phase II. The main design flaw exposed in our Phase II work was the isolation of the volume within the liner from the volume behind the liner (with no means of venting that liner). Helium can diffuse through the liner, over time; but a sudden depressurization of the cycle space causes the liner to bulge or rupture, with no way to relieve that pressure. The newer designs featured first a vent on the outside, and eventually, a change from a captured liner (where the liner is sealed at the ends with a mechanical constraint) to a free liner, where the liner forms an acoustic seal simply by virtue of having an interference fit with the I.D. of the "collars" on the ends of the outside hose, but is not otherwise constrained. This allows any pent-up pressure behind the liner to 'burp' outward. We have adopted this design for our smaller cryocoolers, so although no large FAR systems are envisioned, the transfer line concepts of Phase III are in common use in our products.

The "free liner" construction has worked very well in our small cryocoolers, but experiments with the larger transfer lines showed that 'liner collapse' can still occur, even when the ends of the liner are unconstrained (see Figure 37). Furthermore, this design still uses a silicone liner, which is very difficult to bake dry. More work is required to make the large-diameter flex lines practical.

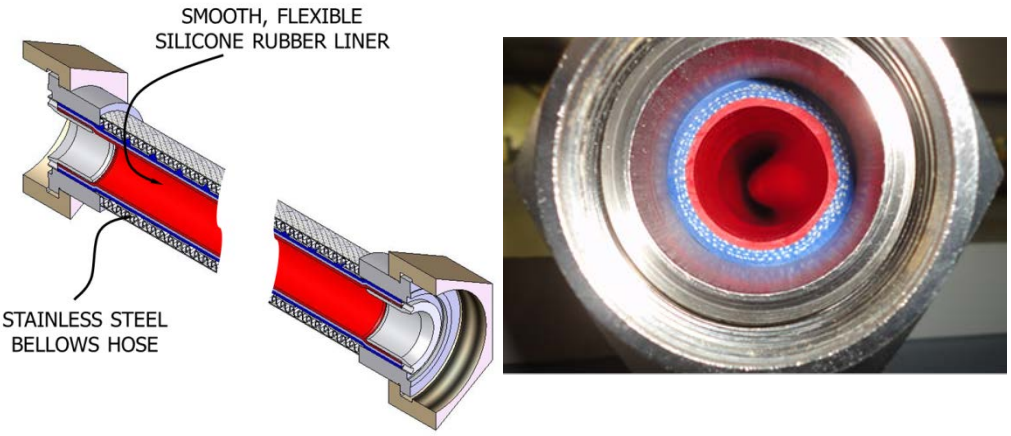

Figure 37: (Left) Original design for large-diameter flex lines, with the liner "captured" by a collar on each end. In this design, high pressure behind the liner can't vent, and any loss of pressure in the cycle space can cause the liner to collapse. (Right) A simplified version, with the liner ends unconstrained—showing that liner collapse can still occur.

Low-cost manufacturing efforts

The Roadmap cost targets were aggressive, to say the least, and we did not meet them nor expect to meet them. We did, however, find a few cost reductions in targeted areas:

1. *Cold Heat Exchanger*. The cold heat exchanger started out (as in the cold-flanged coldhead) with 176 fine slots, of width 0.35 mm. After many redesigns, we ended up with a similar design (sawn slots) but many fewer (only 60) and wider (0.81 mm). This *should* greatly reduce the cost of the CHX, both by reducing the machining time and making it less challenging. Not only is it cheaper to produce the simpler article, but the number of rejected parts would certainly be lower. It was somewhat disappointing, then, that the single article we obtained for the second version was actually *more* expensive than the first ($9436 vs. $8463). The reasons for this are likely twofold:
    a. The price of copper was very volatile during this time, rising from $1.4/lb (commodity price) in 2009 to a high of $4.5/lb in early 2014. This is a commodities market price; the price of actually buying a chunk of copper from a supplier has also been volatile, but doesn't track the commodity price perfectly. A glance back at old McMaster catalogs shows that in the 2012 catalog, the price for a 12″×12″×1.5″ plate of alloy 110 was $214; in December 2016, the online price is $414 for the same piece (while the commodity price of copper has actually fallen in that time). So the raw material was probably more expensive.
    b. While the second design was easier to make, the first piece was essentially impossible. When we received the CHX+cold flange brazement, the fins were so badly bent we had to use shim stock in all 176 slots to straighten and even them out. This was in addition to some places where the piece

was badly torn up instead of having clean saw cuts. We imagine that our supplier underestimated the difficulty of producing the first CHX part, and gave us a more realistic price on the second one. Therefore, the second piece may indeed be easier to manufacture, but doesn't represent a *savings* over what we had so much as a reason to revise *upward* our estimates of producing the first version.

2. *Aftercooler*. As mentioned earlier, the aftercooler used in this work was welded, not brazed, as part of cost-reduction. After receiving this first welded version, we continued working closely with our local master welder, Mark Dwileski (with his company, Northeast Precision Welding), to come up with a second welded version that would be even less expensive. The first aftercooler was made by largely automated TIG-welding; the even-lower-cost version was intended to use resistance welding. Mark's efforts to refine the resistance-welding approach are summarized in his report (Appendix I). The resistance-welding approach never quite came to fruition, but the automated TIG welding (using a CNC machine to position the electrode) looked more and more promising. Figure 38 shows an early test piece next to a refined version of the full-size aftercooler.

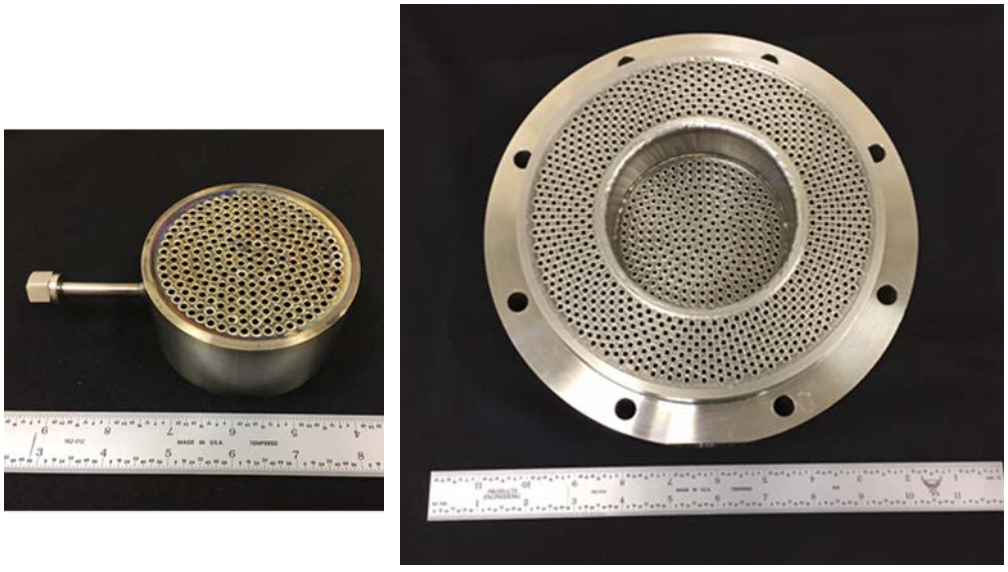

Figure 38: (left) Early welded shell-and-tube sample, followed by refined full-size 362 welded aftercooler (minus some final machining), by Northeast Precision welding.

Based on Mark's estimate for process costs for lots of 10, plus our quotes from vendors for the machined parts, we estimate that the refined-process aftercoolers would cost about $11,000 each in tens/year. It's not clear exactly what benchmark we should compare this against, since the first welded version had no clear process cost (it was development work in progress). To get an estimate, we note that the machined parts alone cost $18,000 (just the parts that comprise the aftercooler, not any of the weld fixturing). We were charged another $11,800 for

the weld-process development that led to the first welded aftercooler. We might guess the cost of welding the first one at half that, or about $5900 (Mark most likely did not charge us for all the time he spent working on the process). Thus we can estimate that the first article cost roughly $24,000. If the cost estimate of $11,000 each for welded aftercoolers in lots of 10 is accurate, this is the most successful single cost-reduction effort in Phase III. We would save over 50% compared to the single-article welded A/C, and perhaps even more compared to what a brazed aftercooler would have cost. We are still using brazed aftercoolers for our "2S241K" coldheads, as our low volume in this product has not been enough to justify Precision Welding investing in the dedicated CNC machines and tooling. Mark did help us come up with an estimated cost for small lots of these for the 241 size, about $3000 each. We are currently paying $9700 each for brazed 241-sized aftercoolers, so the welded version is a major cost savings.

3. *Regenerator*. The regenerator material used in the prototypes is finely woven stainless-steel screen; the raw material is expensive and requires special tooling to punch out to size. The individual screens are very thin and have to be handled very carefully, to avoid creasing them; and because they are so thin, it takes over 1,000 stacked together to fill the regenerator. The alternative, sintered random fiber material (typically used for filtration), is much cheaper per unit area and the raw fiber mat is much thicker than screen (1mm vs. 0.05 mm). The punched (or laser-cut) fiber elements are much easier to handle than screens and there are many fewer of them. Thus, the regenerator is a very obvious target for cost savings. After pricing out random fiber regenerators versus stacked-screen, we still predict significant savings, though with some important caveats:
    a. While the raw fiber mat is definitely cheaper than fine screen, most of the cost of the regenerator elements at the large size and in relatively small quantities (i.e. without ordering thousands of coldheads' worth) is in the processing (the cutting or punching to size) rather than the raw material. In addition, the fiber mats are not available in arbitrary sizes; 400mm×400mm appears to be the maximum size they readily produce (in small quantities). This means the yield per unit area of raw material is lower for the large regenerators, because we can't make as optimum use of the mat area. Overall, we calculate that the random-fiber regenerators (at tens of cryocoolers a year) would cost about $2800/apiece (without labor), versus $5000/apiece for the fine screens, about a 46% savings. In our small (132-size) coldheads, there's more like a 5:1 price difference between screen and fiber, so we don't get quite the same advantage here.
    b. The random fiber will also reduce labor cost and wastage (but these are harder to quantify).

c. The use of random fiber in place of fine screen has been vetted in small coldheads, but we never did verify its fitness for the "362"-size coldhead, since we never quite got the baseline screen version fully functional.

We can estimate based on labor cost alone that packing a regenerator with random fiber is at least eight times faster than packing with fine screens. If we used a burdened labor rate of $100/hour for technician labor (a pretty standard number) that gives us an additional savings of $700 per coldhead.

In addition to these three areas, we pursued lower costs in many of the other parts of the cryocooler. One area in which we were notably not very successful was in reducing the cost of the PWG. This was expected to be a big source of savings, but in quantities of hundreds or even thousands, we did not demonstrate this. The main reasons are:

1. **The stators**, the most expensive part of the motor, would be very inexpensive if made in large quantities, as in tens or hundreds of thousands; they could be sourced from China at a fraction of their current cost. However, this Phase III exercise requires us to find cost savings in relatively small production runs, specifically to get us over the 'valley of death' between research and mass production. We did not find any low-cost vendors that were interested in producing limited quantities of our stators, even overseas.
2. **The enclosing vessel** is the other main component of the PWG that could yield large cost savings, as its subcomponents are all currently machined from full billets of aluminum ("hogged-out," in the vernacular).

   Originally, the idea was to replace the aluminum vessels with welded steel—not stainless steel, but plain steel. It quickly became clear through some basic thermal analysis that the already-borderline heat transfer through the aluminum vessels would be completely inadequate through steel. We briefly pursued keeping the basic aluminum construction, but having the endbells forged rather than machined. Most potential vendors did not have large enough forging presses for our needs, and the tooling required would be very expensive. In addition, the forged blanks would *still* require a fair amount of final machining to make them usable. We considered and discarded several other potential cost-saving constructions. Around the conclusion of this project, we had begun exploring a technique used by our parent company, Chart Industries, in making certain weldments in which a spiral tube is attached to the inside diameter of an enclosing vessel. In our application, the spiral tube would carry coolant inside the pressure vessel, thus enabling the vessel to be made of steel or stainless steel without sacrificing heat transfer. We did not get far enough in this exploration to know if this technique would truly work for us.

Overall, though we did find some significant savings in certain components, we found it extremely challenging to dramatically lower the cost of the overall system in small quantities. Overall, we estimate that in tens per year, we will come in about $100,000 per

core cryocooler (without labor—see Appendix II). Interestingly, this is not far from the first-prototype cost that was presented in our original proposal (about $120,000). We can see now that this cost was greatly underestimated. Thus, while we did find some significant cost savings, we did not move far from the starting line we assumed.

Site Testing

This was supposed to be an important part of the project, originally. Obviously, we did not ever have a full Phase III demonstration system, so no site testing of such a system occurred. We did, however, have a fully functioning cryocooler of the same basic type, just smaller, produced for Phase II. As an alternative to site-testing the Phase III system, we proposed to at least begin by site-testing the Phase II system at our project partner, Superpower, Inc. of Schenectady, NY (now part of Furukawa). This never came to pass. We had immense difficulty getting them to accept the unit for testing, even though they had committed to do so in the contract. Eventually they let us deploy the unit in a test lab, connected to a dewar with a test coil inside (see Figure 39). The early tests indicated that the heat load required to cool their coil was several times more than what they had predicted. Rather than troubleshoot their system, they requested that we retest *our* system, to confirm its performance. We did so, putting the onus back on Superpower to troubleshoot their own piece of the experiment, which they declined to do.

Figure 39: The 2S241K-FAR system developed in Phase II, integrated into a dewar with a test coil at Superpower in Schenectady, NY.

From there, we pursued several other potential sites, but we either could not obtain a commitment in time (Varian expressed interest, but they really wanted a larger system) or could not get permission from the DOE (we had interest from Jereh, a Chinese energy company, but the DOE did not want Government property loaned to China). In the end, then, we did not achieve more than a few weeks of site testing.

Conclusions

To briefly summarize our Phase III effort as it relates to the HTS-4 objectives, we can list our main achievements and our main lessons learned.

Achievements:

1. A 'pulse-tube' coldfinger of record size was designed, built and tested;
2. One full FAR system was built (albeit with a solid transfer tube, not a flexible one)
3. The last few tests indicated that at least 75% of its design capacity was achievable, probably more.
4. Several major components of the coldhead (aftercooler, regenerator, and cold heat exchanger) were redesigned and significantly reduced in cost.

Lessons Learned:

1. The scope of our proposal was a little too ambitious—in particular, the cost targets were not achievable. We would have been wiser to choose one pillar (novelty, performance, cost, or site demonstration) as the emphasis, with the others being secondary.
2. The configuration on which we based our proposal, which required us to develop a record-size coldfinger-style 'pulse-tube' coldhead, does not in fact appear to be advantageous for any real-world application we have encountered.
3. The HTS market was not, as supposed, poised to create high demand for cryocoolers. Even now, in 2016, the HTS market has not matured enough to support significant cryocooler sales.

Regarding this last point, our Phase II final report addressed this same issue, so we have borrowed from that report here. As we phrased it in our Phase II report conclusions [2], DOE support of cryocooler development, including our acoustic cryocoolers, has certainly moved the industry forward and has created new classes of devices and products that are much closer to meeting the Roadmap goals than when the Roadmap was drafted. Maturation of those efforts, however, depends on robust demand for high-temperature superconductors, or some other large-scale market with a similar requirement for cryocooling. Predicting the emergence of markets is always an inexact endeavor; sometimes the actual market far outstrips the predictions, and sometimes anticipated high demand never materializes or is delayed. That is certainly evident in projections of the worldwide market for HTS devices; one example is shown in Figure 40.

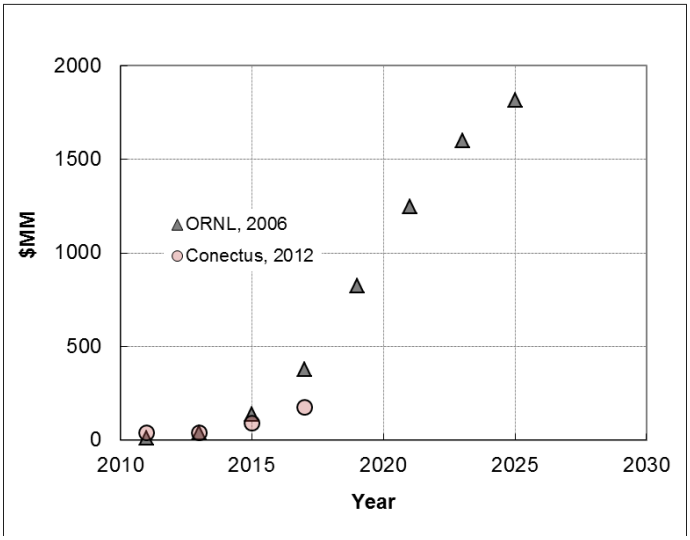

Figure 40: Estimates of the worldwide demand for high-temperature superconductors, from two different sources spaced six years apart.

The triangles show projections from an Oak Ridge National Laboratory Report by Mulholland et al in 2006 [10]; the circles are from a Conectus (CONsortium of European Companies determined To Use Superconductivity) market forecast in 2012 [11]. It is perhaps significant that in the Conectus forecast, the demand is flat for the two years for which comprehensive data were available, but growth was expected subsequently. Still, the growth is much slower than forecast in the ORNL report, which is itself conservative (many reports prepared by superconducting wire makers for their investors project demand for superconducting wire alone will be in the several billions of dollars annually, just a few years hence). Clearly nobody knows at this point if and when a robust demand for HTS cryocooling will occur; at the same time, the current shale oil-and-gas boom was not predicted even a few years before it occurred. Perhaps the fossil-fuel sector will spur demand for on-site natural gas liquefaction, which will in turn help commoditize cryocooling in the capacity range useful to superconducting applications, so that cryocoolers may accelerate the adoption of HTS technology.

Bibliography

[1] M. J. Gouge et al, "Cryogenics Assessment Report," Oak Ridge National Laboratory, http://web.ornl.gov/sci/htsc/documents/pdf/CryoAssessRpt.pdf, 2002.

[2] P. Spoor, "Cost-Effective Acoustic-Stirling Cryocooler with Flexibly Attached Remote Coldhead for HTS," DOE Phase II grant DE-FG02-06ER84646, 2015.

[3] S. A. Potratz et al, " Stirling-type pulse tube cryocooler with 1kW refrigeration at 77K," *Advances in Cryogenic Engineering*, vol. 53A, pp. 42-48, 2008.

[4] R. L. Chen et al, "Reliability Test of a 1kW Pulse Tube for HTS Cable Application," *Advances in Cryogenic Engineering*, vol. 55A, pp. 727-735, 2010.

[5] J. H. So, G. W. Swift and S. Backhaus, "An internal streaming instability in regenerators," *Journal of the Acoustical Society of America,* vol. 120, pp. 1898-1909, 2006.

[6] J. Mulholland, T. P. Sheahen and B. McConnell, "Analysis of future prices and markets for high-temperature superconductors," Oak Ridge National Laboratory, available at: http://web.ornl.gov/sci/htsc/documents/pdf/Mulholland%20Report%20063003.pdf, 2006.

[7] Conectus (CONsortium of European Companies determined To Use Superconductivity), 2012. [Online]. Available: http://www.conectus.org/market.html. [Accessed June 2015].

[8] J. H. Zia, "A pulse-tube cryocooler with 300W refrigeration at 80K and operating efficiency of 19% Carnot," in *Cryocoolers 14*, Boulder, CO, ICC Press, 2007, pp. 141-147.

[9] L. Penswick et al, "High capacity and high efficiency Stirling-cycle cryocoolers," in *Crycoolers 18 (Proceedings of the 18th International Cryocooler Conference)*, Syracuse, NY, 2014.

[10] "ITC Products & Markets," [Online]. Available: http://itcpowersolutions.com/productmarkets.

[11] V. Kotsubo and W. Gully, Separate private communications..

Resulting Products and Technology Transfer

The Phase III effort resulted in some refinements to products in the pipeline, but no new ones were introduced beyond those featured in our Phase II final report [2].

Publications

Our progress in developing the Phase III technology has been reported at several professional meetings, and recorded in conference proceedings:

- P. S. Spoor, “Preliminary Results on a Large Acoustic-Stirling ("Pulse Tube") Cooler Designed for 800W at 70K,” in *Cryocoolers 17*, edited by S.D. Miller and R.G. Ross, Jr. (International Cryocooler Conference, Inc., Boulder, CO, 2012) pp 121-127.
- P. S. Spoor, “Anomalous temperature and amplitude dependent performance characteristic of a 1000W/80K coldfinger,” in *Cryogenic Engineering Conference, Anchorage, Alaska, USA*, p.1405–1409.

Intellectual Property

While some of the particulars about how we build our coldheads and transfer lines are kept "business confidential," we don't consider the type of knowledge that we have gained in this Phase III to be patentable. Coldheads in particular are mostly open art; as a result, this Phase III has not resulted in the creation of new, specific intellectual property.

Glossary of Terms:

2S241K, 2S362K, 2S132K: Model numbers for various QDrive coolers. The three-digit number between S and K is the "frame size" and refers to the diameter of the stator iron in the linear motor of the pressure wave generator, or PWG (see below). In the case of a coldhead, it's the diameter of the stators in the PWG model that would most likely be used to drive a single head.

241, 362, etc. These three-digit codes are used as shorthand to refer to the "frame sizes" above, and may refer to a cryocooler, a PWG, or a coldhead, depending on the context.

Acoustic-Stirling: A type of engine or cryocooler that runs on an approximation of the Stirling cycle, but uses an acoustic network rather than a mechanical displacer.

Buffer tube (or thermal buffer tube): The gas space between the cold heat exchanger and secondary warm heat exchanger in an acoustic-Stirling cryocooler; when configured properly, the gas in the buffer tube undergoes plug flow, serving to enforce the proper cycle phasing in the cooler and insulate the cold zone from the warm zones. Often called a "pulse-tube" for historical reasons.

CFD: Computational Fluid Dynamics.

CHX: Cold heat exchanger.

FAR: Flexibly Attached Remote—a cryocooler with a pressure-wave generator and coldhead connected by a long, flexible transfer line.

HHX: Hot heat exchanger (in a cryocooler or refrigerator, "hot" generally means "ambient", i.e. the heat-reject temperature).

PWG: Pressure Wave Generator—the acoustic power source that drives the cryogenic cooling cycle in an acoustic cryocooler. Sometimes called a "compressor" in the industry (or "linear compressor" to distinguish it from a valved compressor, which provides steady flow instead of oscillating flow).

Piston Drift: The tendency for a free piston (one not constrained by a crankshaft, as in automobile engines or kinematic Stirlings) to oscillate about a mean position displaced from its nominal equilibrium, due to an imbalance of time-averaged pressure on the two sides of the piston. In the case of free pistons with clearance seals, this arises from the slightly asymmetric mass flow of the working fluid through the seal in the two halves of the cycle. This "piston drift" typically reduces available capacity by shortening the useful stroke (there is normally a stroke limit to a free piston determined by flexure stress).

Pulse Tube: A term of art referring to a class of cryocoolers that use a passive acoustic network in place of a mechanical displacer to approximate the Stirling cycle, or to a component of those cryocoolers (see "Buffer tube").

pV power: Work done on a gas by a pressure source; the integral of $p \cdot dV$, where p is pressure and V is volume. In an acoustic system, it is generally synonymous with acoustic power.

APPENDIX I

Report prepared by Mark Dwileski on progress developing a weld process for the large aftercoolers.

NORTHEAST PRECISION WELDING, INC.

P.O. BOX 109 EAST GREENBUSH, NEW YORK 12061 PHONE (518) 441-2260/ FAX (518) 479-4010

February 1, 2012

Dr. Phil Spoor
Mr. David Lala
Clever Fellows
CFIC, INC.
302 Tenth St.
Troy, NY 12180

Re: Summary Report – Alternative Welding Options

Dear Phil and Dave:

Northeast Precision Welding, Inc. is pleased to have explored an alternative welding option for the Aftercooler Weldment.

The current method of welding the tube to sheet connections was conducted using a micro pulse tig arc to seal weld each tube. The goal is to explore welding options that can significantly reduce weld time while maintaining the quality of the tig weld.

The first efforts were directed to resistance welding. A tungsten electrode was centered into the tube end followed by an electrical charge. The experimental components were the tungsten pressure and current levels. As the current levels were raised, fusion of the weld connection favored the tight side of the weld joint connection, resulting in incomplete fusion. The realistic tube diameter, tube hole diameter and out-of-roundness tolerances may be detrimental factors to achieve repeatable reliable seal welds.

The focus was steered toward a rotating tapered tungsten electrode combined with controlled pressure. This formed the tube end to match the tube sheet hole. A current charge was applied then the tungsten electrode released and repositioned to the next connection etc. The attached pictures show the results of this process. More effort and research will be needed to implement this alternative welding option and to be considered reliable.

We look forward to continuing this welding R&D and aiding in the development of an economical Aftercooler Weldment.

Please call me if you have any questions.

Very truly yours,

M. Dwileski

Mark D. Dwileski, Jr.

APPENDIX II

Detailed cost estimates for producing 2S362K-FAR's in lots of 10.

			$99,556.99
Component Part	Component Desc	BOM Qty Total	Estimate Total Part
2S362K-18992-A	Aftercooler, Weldment (incl 18996,18997,18998)	1	$ 5,750.00
2S362K-19002-C	Ring, Aftercooler Weldment	2	$ 1,596.00
2S362K-18994-C	Plate, Core, Aftercooler Weldment	2	$ 1,260.00
2S362K-19003-C	Baffle, Aftercooler Weldment	1	$ 965.00
2S362K-19000-A	Aftercooler, Machined	1	$ 685.00
2S362K-18995-C	Housing, Aftercooler Weldment	1	$ 323.40
2S362K-18999-A	Tube Sheet, Core, Machined	1	$ 285.00
2S362K-18993-C	Internal Wall, Aftercooler Weldment	1	$ 80.95
2S362K-19013-A	Water Connection Assembly, Aftercooler	1	$ -
2S362K-19010-C	Block, Water Connection, Aftercooler	1	$ -
2S362K-19018-C	Gasket, Water Connection to Coldhead	1	$ -
2S362K-19025-C	He Tube, Plate Support, Aftercooler Weldment	1	$ 165.00
	AFTERCOOLER TOTAL:		$11,183.70
2S362K-18978-C	Regenerator, Copper	18	$ 1,800.00
2S362K-18836-C	Regenerator, Bottom	714	$ 1,386.00
2S362K-18977-C	Regenerator, Top	480	$ 1,386.00
2S362K-18838-C	Regenerator, Coarse	4	$ 48.00
	REGENERATOR TOTAL		$4620
	RASP Box	1	$ 9,600.00
2S362W-13074-C	END VESSEL - 362 LW	2	$ 4,514.80
2S362W-13077-C	CENTER BODY - 362 LW	1	$ 4,401.61
P01954	PowerFlex 700 AC Drive, 125A, 480VAC, Frame 5 (Allen-Bradley 20BD125A3ANNANC0)	1	$ 7,925.00
1S362M-13076-C	CROWN RING - 362 LW	2	$ 6,380.00
1S362M-16007-C	STATOR - 362	2	$ 2,301.11
2S362W-13078-C	PISTON SLEEVE, 362 LW	2	$ 4,570.00
2S362W-13092-C	PISTON, 9.70 O.D. 362 LW	2	$ 4,100.00
2S362K-18863-C	Extension, Front Volume (Chimney)	1	$ -
2S362K-18832-C	Housing, Regenerator	1	$ 3,165.00
2S362K-18834-C	Cold Heat Exchanger	1	$ 3,165.00
1S362M-13075-C	STRAP RING - 362 LW	2	$ 3,020.00
2S362K-18979-C	Junction, Coldhead to Remote Inertance Tank	1	$ 2,686.50
2S362W-13647-C	COVER, FRONT VOLUME, 362 LIQUEFIER	1	$ -
2S362K-18982-C	Stack, Sintered Wire Cloth, Cold Flow Straightener	1	$ 1,800.00
2S362K-18981-C	Stack, Sintered Wire Cloth, Warm Flow Straightener	1	$ 1,800.00
2S362K-18000-A	Cabinet Assy	1	$ 1,766.35
P00335	Endevco Signal Processor	1	$ -
2S362K-18862-C	Blank Cap, PWG Chimney	1	$ 1,165.00
P01874	SENSOR, POSITION VIP, 50 mm RANGE, THD HSG (MICRO EPSILON VIP-50-GA-5-SA7-I)	2	$ 1,062.00

2S362K-18853-C	Fitting, Transfer Hose	2	$ 1,030.00
P00832	Piezoresistive Pressure Transducer, 500 psia, sealed, with 30 inch long cable	1	$ -
P01963	METER, 2 Relays 3 A @ 240 Vac, Form C SPDT, OMEGA CNi8DH53	3	$ -
2S362K-13649-A	Cart Assy	1	$ 1,000.00
2S362K-19019-A	Inertance Tank Weldment	1	$ 992.00
2S362W-13068-C	SUPPORT FOOT, PWG - 362 LW	2	$ 930.00
1S362M-16006-C	FLEXURE, DIAMETRAL .024 THK, 362 FRAME	16	$ 875.68
2S362K-18852-C	Coldhead Clamping Flange	1	$ 810.00
2S362K-18984-C	Flow Straightener, Warm	1	$ 800.00
2S362K-18983-C	Flow Straightener, Cold	1	$ 800.00
2S362K-18980-C	Buffer Tube	1	$ 785.00
2S362K-18976-C	Hose, Helium Containment, Transfer	1	$ 593.75
2S362K-20141-A	ASSY, CRYOCOOLER REQUIRED AUXILIARY PARTS 362	1	$ 550.00
1S362W-17533-A	MOTOR PISTON ASSEMBLY, CUT, 362	2	$ 495.00
2S362K-13650-A	TRANSFER INTERFACE FITTING - 362 3 HEAD LIQUEFIER	3	$ -
1S362M-16043-C	CABLE ASSEMBLY MOTOR FEED THRU (Douglass P/N 45443-OR)	2	$ 442.00
1S362M-17527-A	STATOR ASSEMBLY, 362 FRAME, 380 VOLTS	2	$ 425.00
2S362W-18017-C	ANTI DRIFT TUBE, 362 LW	1	$ 425.00
2S362W-13073-A	PWG ASSEMBLY, 9.70 PISTON - 362 LW	1	$ 425.00
P01945	WIRE, 2AWG, 4COND HARSH ENVIRONMENT CABLE	34	$ 418.20
P02026	OUTPUT LINE REACTOR ALLEN BRADLEY P/N 1321-3R130-B	1	$ -
1S362M-20090-C	MAGNET, 362 1.500 CUBE N48M EPOXY COATED	32	$ 384.00
P01496	NEWPORT ELECTRONICS INC - I8C00 - Process/Temperature Controller	1	$ -
1S362M-17529-A	STATOR ASSEMBLY, VPI, 362	2	$ 350.00
P01965	METER, 3 CHANNEL TEMP, OMEGA DP472-T-C2	1	$ -
P01964	METER ANALOG 0-10vDC, OMEGA CNi8DH33	1	$ -
P01078	Industrial vibration sensor, 4-20mA output, 0 to 5 g s RMS, 3 to 1000 Hz, 1/4-28 tap mounting hole, supplied with integral 10 ft cable-cf connector 2 skt mil c5015 plug molded	1	$ 335.00
1S362M-13067-C	SPACER, FLEXURE - 362 LW	16	$ 313.28
2S362K-18850-C	Flow Turning Vane, Middle	1	$ 285.00
2S362K-18849-C	Flow Turning Vane, Top	1	$ 285.00
2S362K-18855-C	Turning Vane, Bottom	1	$ 285.00
2S362W-16087-C	CABLE ASSEMBLY THERMOCOUPLE FEED THRU	1	$ 282.00
1S362M-21173-A	MAGNET, EPOXY COATED 362 FRAME	16	$ 240.00
P02025	POWER SUPPLY, 24V, 120W DIN MOUNT, ALLEN BRADLEY 1606-XL120D	1	$ -
P02025	POWER SUPPLY, 24V, 120W DIN MOUNT, ALLEN BRADLEY 1606-XL120D	1	$ -
P01868	cable for VIP-100/50 etc. (MICROEPSILON C703-5)	2	$ 210.00
1S362M-17537-A	COIL ASSEMBLY FOR 362	16	$ 204.00
1S362M-12436-00-C	SPIDER, MAGNET 362	4	$ 192.00
P00541	TUBING, TYGON PVC, BRAID-REINFORCED .625 ID X .875 OD, 2.375 BEND RADIUS	40	$ 185.60
1S362M-12437-00-A	MAGNET CORE ASSEMBLY - 362 FRAME	2	$ 170.00
2S362W-13999-A	FILL PORT AND ANTI DRIFT CIRCUIT - 362 LW PWG	1	$ 170.00
2S362K-19040-A	Transfer Hose Assembly, 2m Length	1	$ 160.00
1S362M-12445-00-C	CLAMP BAR - 362 FRAME	32	$ 153.60
P00347	1/4 tube, relief valve, 3XX SS	1	$ 144.43
P01536	VALVE, BELLOWS SEALED, 1/4 TUBE FITTING	1	$ 143.00
P01974	UL Class J Time-Delay Fuse 600 VAC, 100 Amps, Fuse Types: Lpj-SP, Ajt, Jtd	3	$ -

P02062	CABLE, 6AWG, SHIELDED, 4 CONDUCTOR 1000VAC	10	$ 142.00
2S362W-13069-C	CENTER AXIS SCREW	2	$ 141.36
P01968	TRANSFORMER, 240_480 PRI 120 SEC, 500VA, McMASTER 6988K36	1	$ -
2S362W-16080-C	LOCK, FEED THRU SEAL	1	$ 132.00
2S000K-19042-A	Modified Enclosure for -IP Pressure Signal Processor	1	$ -
2S362W-13097-A	PISTON RULON ASSY, 9.70 OD - 362 LW	2	$ 112.00
P02449	HOSE, SILICONE, 1.75ID, 2.125OD, 23 BEND RADIUS, 3 PLY, POLYSETER BRAID RE-ENFORCED, RED ID, BLUE OD	6.67	$ 97.72
P01098	NAS Bolt, 1/4-28 UNF-3A x 1.312 grip length, Alloy steel, cadmium plated	32	$ 96.00
P01881	TUBING, COPPER, CLEANED & CAPPED 3_8 OD X .032 W 100 FT McMASTER 5174K35	66	$ 92.97
2S362W-16086-C	BLOCK, THERMOCOUPLE SEAL - 362 FRAME	1	$ 90.74
P02362	AC-DC power supply; + - 15 VDC nominal output; 0.15 amps output current (ACOPIAN D15-15A)	1	$ 90.00
1S362M-12435-00-C	CORE, MAGNET 362	2	$ 86.00
1S362M-17535-A	STRAP RING ASSEMBLY 362 LW	2	$ 85.00
1S362M-17531-A	MOTOR ASSEMBLY, 362	2	$ 85.00
1S362M-17530-A	STATOR ASSEMBLY BAKE-OUT AND INSPECT	2	$ 85.00
2S362W-13070-C	BULKGHEAD FITTING SUPPORT - 362 LW	2	$ 84.64
2S362W-13057-C	CAP, POSITION SENSOR MOUNTING - 362LW	2	$ 76.70
1S362M-16009-C	FLEXURE, DIAMETRAL - BEND - 362 FRAME	16	$ 71.36
2S362K-13413-A	MODIFIED SWAGELOK FITTING FOR 3 HEAD LIQUEFIER	3	$ 68.10
P01454	EYEBOLT, SHOULDER - FORGED ALLOY STEEL, 1/2-13X1 1/2 FULLY THREADED	4	$ 65.52
2S362K-18022-A	LABELS- CONTROL 362 3 HEAD LIQUEFIER	1	$ 65.00
P01879	SCREW, SHCS, Stainless Steel, 5/16-18 X 7.OO LG	14	$ 63.70
P01100	Screw, SCHD, 18-8 SST, 10-24 x 5.0	19	$ 63.65
P01972	UL Class Fuse Block Class J, 600 VAC, 3-Pole, 61-100 Amps	1	$ 62.82
1S362M-10618-C	CLAMP, COIL 362 FRAME	16	$ 59.04
P01976	HIM BEZEL ALLEN BRADLEY 20-HIM-B1	1	$ 57.20
2S362W-13096-A	RULON, 362 LW	2	$ 57.00
1S362M-17532-A	MOTOR PISTON ASSEMBLY, 362	2	$ 56.10
2S241K-17592-C	FITTING, 5/8 ID HOSE, BARBED X SOLDERED	2	$ 55.74
P02229	HANDLE, OVAL GRIP, 5-13/64 CTR TO CTR 1/4 HOLES	3	$ 52.50
P02057	WIRE, 12AWG 600VAC STRANDED, BLACK PER UL1015	100	$ 51.66
P01966	EMERGENCY STOP , 40mm RED AB 800FP-MP44PX01S	1	$ 51.62
1S362M-17528-A	SURGE RING, 362 FRAME, 380 VOLTS	2	$ 45.00
P01978	GRAB BAR, STAINLESS 36 INCH MCMASTER 2823K47	1	$ 44.22
2S000K-18963-C	PCB for -IP Pressure Signal Processor	1	$ -
1S362M-12505-00-C	WASHER, BEARING - 362 FRAME	2	$ 42.78
2S362W-17534-A	MOTOR PISTON ASSEMBLY, FINAL - 362 LW	2	$ 42.50
2S362W-16103-C	BOX, ELECTRICAL JUNCTION - NEMA 3R	1	$ 42.50
P00358	1/4 tube, Union Cross, 3XX SS	1	$ 39.60
P01820	THERMAL EPOXY, EPOXIES ETC P/N 50-3100, pint	1	$ 39.01
P01979	GRAB BAR, STAINLESS 24 INCH MCMASTER 2823K35	1	$ 38.00
1S362M-12439-00-C	LINER, STRAP - 362 FRAME	8	$ 37.52
P00133	Nut, Cinch, 12 pt Hex, 3/4-16, Alloy Steel	1	$ 37.50
5174K12	Cleaned and Capped Copper Tubing 3/4" Tube Sz, 7/8" OD, .785" ID, .045" Wall, 50' Coil	10	$ 33.81
P02366	Enclosure, Electronics, Aluminum Body, Black ABS Trim, 3.27X6.27X7.06 (Bud Industries EX-4522)	1	$ -

P02060	WIRE, 14AWG 600VAC STRANDED, WHITE PER UL1015	100	$	32.51
P02058	WIRE, 14AWG 600VAC STRANDED, RED PER UL1015	100	$	32.51
P02444	Standoff, Hex, Male-Female, Zinc-Plated Steel, 1/2 Hex x 1-1/2 Length, 1/4-20 Screw Size	6	$	31.44
2S362W-13071-C	BULKGHEAD FITTING MOUNT - 362 LW	2	$	30.42
P00833	ENDEVCO WIRE 24328	6	$	30.00
P01929	TEE, SST 1_2 MICROGROUP 30FF-8	2	$	29.86
P01927	BULKHEAD FITTING, SST, 1_2 TUBE SWAGELOK SS-810-61	1	$	29.52
P01958	DISCONNECT SWITCH, 480V, 100A ENESTO, KSR3.100	1	$	29.50
P02059	Thermocouple, type E, .062 dia, 18in stainless probe length, ungrounded junction	1	$	27.60
P00293	Screw, SCHD, 18-8 SST, 1/4-20 x 4 1/2	4	$	27.20
P00346	Rulon J, .062 thk x 4.00" wide (TOS) Treated one side	34	$	26.38
P01876	BULKHEAD FITTING .375 TUBE BRASS, SWAGELOK B-600-61	4	$	26.00
P02065	ADAPTOR, TERMINAL BLOCK TO DIN RAIL	30	$	25.20
1S362M-10617-00-C	BOBBIN, COIL - 362 FRAME	16	$	24.00
P00473	Thermocouple, type K, with self-adhesive pad	2	$	24.00
P01983	UNION, REDUCING, SST 1/2 TO 1/4 TUBE	1	$	23.60
P01973	UL Class Fuse Block Safety Cover Indicating, for Class J (600 VAC), 65-100 Amps	3	$	23.46
P01821	CATALYST 190	1	$	22.85
2S362K-19029-A	Assembly, Buffer Tube - Flow Straighteners	1	$	22.50
2S362K-19026-A	Regenerator Housing & TC Assembly	1	$	22.50
P02061	WIRE, 16 AWG 600VAC STRANDED, BLUE PER UL1015	100	$	22.22
P01490	TB4M; Connector for Endevco	2	$	22.20
P02067	FUSE HOLDER, DOUBLE POLE, DIN MOUNT, CLASS CC FUSE 30A 600V	1	$	-
P01928	REDUCING UNION, SST 1_2 TO 3_8 MICROGROUP 5FF-8-6	2	$	21.76
P01479	STUD, FULLY THREADED, 5/8-11 X 6 LONG, GRADE B16	6	$	20.58
P02063	TERMINAL BLOCK, 4 CIRCUIT, DIN MOUNT 20 AMP AT 300VAC	10	$	-
P02068	FUSE, UL Class CC, 1-1/2 AMP, 600VAC TIME DELAY	2	$	20.04
P01409	Copper Tubing, Alloy 122, 1/4 Tube Size, 3/8 OD, .277 ID, .049 Wall Thk	108	$	19.26
P00039	1/16 tube, Male fitting, 5/16 SAE, 3XX SS, face seal, bored thru, Swagelok SS100-1-ORBT	1	$	18.92
P01990	RELAY, 230VAC COIL, DOUBLE POLE AB P/N 700-HA32A2	1	$	18.72
P01961	DIAL, 10 TURN POTENTIOMETER, VISHAY 11-1-11	1	$	18.66
P01501	SCREW, HHCS, 5/8-11 X 5, GRADE 8	28	$	18.37
P01962	POTENTIOMETER, 10 TURN, 10K, 5%, 2W HONEYWELL 73JA10K	1	$	18.27
P00225	1/4 tube to 1/2 tube fitting reducer, 3XX SS	1	$	17.70
P01912	Rain-Tight Outdoor Steel Enclosure (NEMA 3R) with Knockouts, Screw Cover, 8 H X 6 W X 4 D	1	$	17.56
P01951	Garden Hose-to-Pipe Rigid Connectors 3/4 Male Garden Hose, 1 NPT Male Connections	2	$	17.42
P01484	AD621ANZ; Amplifier ; 18.0V max supply; Supply Voltage Min.: 2.3V	2	$	17.28
P02424	Epoxy, Thermally Conductive, 9.6 (BTU•in)/(hr•°F•ft^2), Black, 2 Parts	1	$	17.00
P01971	BNC CONNECTOR, FEMALE TO FEMALE BULKHEAD FITTING POMONA 3846	2	$	16.00
P01995	BARBED FITTING, 5/8 ID TUBE X 1/2 MNPT	8	$	15.49
P00374	SST Tubing, Type 316, 1/2 OD, .402 ID, .049 Wall Thk.	2	$	14.96
P01982	ADAPTER, 1/4 TUBE TO 7/16 SAE MALE, SAWGELOK SS-4-TA-1-4ST	2	$	14.40
P01097	NAS bolt, HHMS, 10-32 x .375" grip	24	$	14.40
2S362W-16085-C	GROMMET, ELECTRIC JUNCTION BOX	1	$	14.16
P02443	Stud, Steel, 3/8-16 X 8.0, Black-Oxide, Threaded 1.25 Both Ends	8	$	13.92
P01993	Low-Pressure Brass Threaded Pipe Fitting 1 INCH Pipe Size, Square Socket Plug	2	$	13.64

2S241W-11648-00-C	LABELS, GENERIC PRODUCT	1	$	13.18
P00834	TA4F CONNECTOR FEMALE RECEPTACLE	2	$	13.01
P00269	1/4 tube port connector, 3XX SS	2	$	11.00
P02066	FUSE HOLDER, SINGLE POLE, DIN MOUNT, CLASS CC FUSE 30A 600V	1	$	10.67
P01481	NUT, HEX, 5/8-11, GRADE 8, ZINC PLATED	42	$	10.25
P02064	TERMINAL BLOCK, 2 CIRCUIT, DIN MOUNT 20 AMP AT 300VAC	10	$	10.00
P00567	miniature connector for type K thermocouple, female, w/ write-on window	4	$	9.00
P01930	REDUCER, SST 1/2 TO 3/8 MICROGROUP 5MF-8-6	1	$	8.80
P01416	O-RING, BUNA-N, 2-460	2	$	8.37
P01485	VOLTAGE REFERENCE, TO-5 PACKAGE, ANALOG DEVICES AD581	1	$	8.32
P01960	DOOR MOUNT KIT FOR DISCONNECT SWITCH ,ENESTO KSED3	1	$	8.00
P02074	BLOCK, CONTACT SCREW DOWN	1	$	7.84
P01947	SCREW, SHCS ALLOY ST, 3/8-24 X 1.25 McMASTER 91251A426	24	$	7.61
P00221	Screw, SCHD, 18-8 SST, 10-24 x 2 3/4	8	$	7.47
P00725	1/2 tube plug, 3XX SS	1	$	7.10
P02021	ELBOW, 90DEG 1 CONDUIT FITTING,DIE CAST ZINC	1	$	6.82
P00509	CONNECTOR,BRASS .25 TUBE X .43 SAE, SWAGELOK B-400-1-4ST	2	$	6.76
P01880	DOWEL. 18-8 .375 OD X 1.25 LG McMASTER 90145A626	4	$	6.48
P02450	Sheet, Copper, .032 Thick, Annealed	0.25	$	6.48
P02028	SCREW, SHCS ALLOY ST, 3_8-24 X 3.25	6	$	6.36
P01991	RELAY SOCKET, AB P/N 700-HN125	1	$	6.23
P02368	Cord, Power, 9'10", NEMA 5-15 to IEC 320, SJT, 18-3, .32 Diameter Wire	1	$	6.14
P02075	BUTTON, PUSH PLASTIC	1	$	5.89
P00032	1/4 tube, Plug, 3XX SS	1	$	5.30
P01480	STUD, FULLY THREADED, 5/8-11 X 5 LONG, GRADE B16	2	$	5.12
P01959	HANDLE,FOR DISCONNECT SWITCH, ENESTO KSH48RY	1	$	5.00
P02069	FUSE UL Class G, 3A,600VAC FAST ACTING	1	$	4.75
P00205	Screw, SCHD, Alloy Steel, 3/8-16 x 1 1/2	16	$	4.27
P02009	SCREW, SHCS ALLOY ST, 3_8-16 X 3.00	6	$	3.94
P00348	Spring kit, 350 to 750 psig	1	$	3.90
P02179	CONNECTOR, BNC PANEL MOUNT, SOLDER CONNECTIONS	2	$	3.80
P02365	Terminal Block, 4 Position, 5mm Pitch (Pheonix Contact 1715048)	2	$	3.72
P01494	POWER ENTRY MODULE, EIC, FUSED (Schurter 6200.2100 or 6200.2300)	1	$	3.53
P01188	Screw, Hex Hd, Grade 8 Zinc-Plated Steel, 5/8-11 x 1 1/2	4	$	3.50
P01988	Black-Oxide Steel Both-Ends Threaded Stud Round Shank, 1/4 -20 Thread, 8 Overall Length	2	$	3.30
P02204	INSERT, HELICAL THREAD, 18-8 STAINLESS STEEL, 1/4-20 X .375 LONG, WITH TANG (McMaster 91732A212)	8	$	3.20
P01415	O-RING, BUNA-N, 2-275	2	$	3.19
P00418	Washer, Flat, 18-8 SST, 3/8 AN, .390 ID,.625 OD, .057-.069 Thk,	30	$	3.08
P00566	miniature connector for type K thermocouple, male, w/ write-on window	2	$	3.02
P01477	WASHER, LOCK, SPRING STEEL, 5/8	36	$	2.75
P00215	Screw, SCHD, Alloy Steel, 3/8-16 x 1 3/4	8	$	2.54
P00460	Screw, SCHD, Alloy Steel 3/8-16 x 2 1/4	8	$	2.48
P00113	Dowel Pin, 316 SST, 1/8 dia. x 1/2	4	$	2.46
P00203	Screw, SCHD, Alloy Steel, 1/4-20 x 1 1/4	16	$	2.24
P00953	Buna-N rubber tubing, 1/4 ID x 3/8 OD, 1/16 Wall Thk.	24	$	2.11
P02363	Terminal Block, 2 Position, 5mm Pitch (Pheonix Contact 1715022)	2	$	1.90
P01410	Screw, BTNHD, 18-8 SST, 1/4-20 x 1 1/2	8	$	1.86

P01956	COUPLING, 5/8 ID HOSE, BARBED, BRASS (McMaster 91355K86)	1	$	1.60
P00820	Din 3 Rail, Steel, 35mm. Width, 7.5mm. Heigth, 1m. Lg.	0.25	$	1.50
P00125	Washer, Flat, 18-8 SST, 1/4 NAS, .255 ID, .468 OD, .060-.066Thk,	20	$	1.43
P00437	Glass fuse, 500mA, GDC series, time-lag, 5mm x 20mm	1	$	1.42
P02364	Terminal Block, 3 Position, 5mm Pitch (Pheonix Contact 1715035)	1	$	1.42
P02020	SCREW, OVAL HEAD, 18-8SST, 10-32 X .50 LG MCMASTER 91802A829	12	$	1.23
P01948	O-RING, BUNA-N, 2-266	1	$	1.17
P01948	O-RING, BUNA-N, 2-266	1	$	1.17
P01873	ROD, NYLON, 6/6, .250 INCH DIAMETER	34	$	1.11
P01877	SCREW, SHCS ALLOY STEEL,1_4-20 X 2.75 McMASTER 91251A553	4	$	1.08
P00342	Screw, SCHD, Alloy Steel, 1/4-20 x 3/4	9	$	1.07
P00327	Locknut, Hex, Nylon-Insert, 316 SST, 10-32	12	$	1.03
P01488	470 Ohms Resister;	1	$	1.03
P02367	Standoff, Aluminum, 4-40 Threads, .19 Male, .13-.25 Female, .38 Body Length, .25 Hex	2	$	1.02
P01923	SCREW, HHCS GR5 STL 1/4-20 X .5O MCMASTER 92865A537	24	$	0.98
P00117	Washer, Flat, 18-8 SST, #10 NAS, .195 ID, .354 OD, .060-.066 Thk,	16	$	0.88
P01161	Screw, Pan Hd Mach w/ Dual-Action Spring Washer, 18-8 SST, 4-40 x 1/4	2	$	0.86
P01289	O-RING, BUNA-N, 2-261	1	$	0.85
P00474	Tubing, .375" dia x .035" wall, 316 / 316L SS, Seamless, 20 ft length	0.3	$	0.84
P01925	SCREW BHSHCS,SST BLK 1-4-20 X .50 LG McMASTER 97763A263	2	$	0.80
P00145	Screw, SCHD, Alloy Steel, 1/4-20 x 1.0	6	$	0.79
P01476	WASHER, FLAT, 5/8	8	$	0.76
P01414	O-RING, BUNA-N, 2-260	1	$	0.76
P00101	O-RING, BUNA-N, 2-262	1	$	0.76
P02072	VARISTER, 230Vrms LITTLEFUSE V230LA20AP	2	$	0.75
P02085	SLOTTED SPRING PIN, 420 SST 7/32 DIA X 2.75 LG	1	$	0.74
P00883	Screw, SCHD, Alloy Steel, 8-32 x 5/8	6	$	0.70
P00204	Washer, Flat, Zinc-Plated Steel, 3/8 SAE, 13/32 ID, 13/16 OD, .055-.072 Thk,	8	$	0.69
P00135	Locknut, Hex, Nylon-Insert, 316 SST, 10-24,	8	$	0.69
P00734	Washer, Spring Lock, 18-8 SST, 1/4, .26 ID., .363 OD., .078 Thk.	16	$	0.66
P01473	SCREW, BHCS, 1/4-20 X .500, 18-8 SS	4	$	0.61
P02008	SCREW, SHCS ALLOY ST, 3_8-24 X 1.00 McMASTER 91251A424	2	$	0.59
P01486	2N6040; BJT Transistor; Current Rating: 8 A	1	$	0.58
p01751	SCREW, SHCS, ALLOY ST,10-32 X 1-1/2 LG McMASTER 91251A351	4	$	0.56
P02210	INSERT, HELICAL THREAD, 18-8 STAINLESS STEEL, 8-32 X .328 LONG, WITH TANG (McMaster 91732A713)	1	$	0.56
P00349	Screw, SCHD, Alloy Steel, 3/8-16 x 1.0	2	$	0.47
P00626	Bumper, Recessed Rubber w/o Washer, SBR, 5/16 ID top, 5/32 ID Bottom	4	$	0.37
P01413	O-RING, BUNA-N, 2-120	8	$	0.36
P00425	NUT, HEX, Grade 8, 3/8-16, .56 Width X .33 Thick	8	$	0.34
P00866	Washer, Spring Lock, Zinc-Plated Steel, 3/8, .385 ID, .680 OD, .094 Thk	8	$	0.27
P00152	Screw, SCHD, Alloy Steel, 10-24 x 1.0	2	$	0.24
P01941	O-RING, BUNA-N, 2-165	3	$	0.24
P00137	Locknut, Hex, Nylon-Insert, 18-8 SST, 6-32	4	$	0.21
P00628	Screw, SCHD, 18-8 SST, 6-32 x 5/8	4	$	0.20
P01987	Durable Black Neoprene Rubber Tubing 1/4 ID, 1/2 OD, 1/8 Wall Thk	2	$	0.19
P02390	O-RING, BUNA-N, 2-239	1	$	0.19
P01914	O-RING, BUNA-N, 2-034	2	$	0.17
P00483	Wire, #11 (2:1) rectangular magnet wire .091x.182, 16116 sq mils	1	$	0.16

P02435	Screw, Pan Head Philips Machine, Brass,8-32X.75 Long	1	$	0.16
P00822	O-RING, BUNA-N, 2-043	1	$	0.16
P00126	Washer, Flat, Steel, 3/4 SAE, 13/16 ID, 1 15/32 OD, .108-.160 Thk,	1	$	0.15
P02136	O-RING, BUNA-N, 3-932	1	$	0.15
P02441	O-Ring, Buna-N, 2-044, Shore A: 70	1	$	0.14
P00829	Screw, SCHD, Alloy Steel, 10-32 x 5/8	2	$	0.14
P01934	EDGE TRIM, POLYETHYLENE 1/16 OPENING X 13/64 LONG	0.8	$	0.14
P01924	WASHER, 18-8 SST,BLACK 1_4 McMASTER 96765A140	2	$	0.14
P01165	RING TERMINAL, 22-18 AWG, #6 STUD	1	$	0.13
P01335	O-RING, BUNA-N, 2-216	2	$	0.12
P00297	Screw, SCHD, 18-8 SST, 6-32 x 1.0	2	$	0.12
P01487	Capacitor, 0.250 inch Lead Space, 0.1 micro F	1	$	0.12
P00094	O-RING, BUNA-N, 2-214	2	$	0.11
P00120	Washer, Flat, 18-8 SST, #6 NAS, .143 ID, .267 OD, .029-.035 Thk,	4	$	0.10
P00182	Rivets, Blind, Dome Style, ALUM, 1/8 dia. X .188-.250 Thk	4	$	0.09
P02451	Sheet, Buna-N, 40A Durometer, .06 Thick	1	$	0.08
P00492	Washer, Flat, 316 SST, #10, 13/64 ID, 7/16 OD, .032 Thk,	2	$	0.07
P00533	Washer, Spring lock, 18-8 SST, #10, .200 ID, .334 OD, .047 Thk (McMASTER 92146A550)	4	$	0.06
P00407	Rivet, Blind, Dome Style, Alum, 1/8 dia., .126-.187 Thk	2	$	0.05
P02442	O-Ring, Buna-N, 2-121, Shore A: 70	1	$	0.04
P01767	WASHER, LKG, INT TOOTH ZN PL STEEL #10	1	$	0.02
P00608	Washer, Spring Lock, Zinc Plated Steel, #6, .148 ID, .250 OD, .031 Thk	2	$	0.01
2S362K-18835-A	Coldhead, Coax, Side Port	1	$	-
2S362K-18833-A	Regenerator Housing Brazement	1	$	-